Plant Communications
Research article

CellPress
Partner Journal

Prime editing of an RR26-responsive *cis*-element enhances *DAHPS2* expression and submergence tolerance in rice through the shikimate pathway

Dongdong Chen[1,7], Linlin Hou[1,7], Zhennan Qiu[4,7], Qiang Xu[5], Qiaoyan Wang[1], Man Li[1], Zhiqi Hao[1], Pengfei Dong[1], Guangheng Zhang[1], Jiang Hu[1], Zhenyu Gao[1], Guojun Dong[1], Deyong Ren[1], Lan Shen[1], Yuchun Rao[6], Qing Li[1], Yuhang Zhang[1,3], Qiang Zhang[1], Longbiao Guo[1], Lianguang Shang[5,*], Qian Qian[1,2,3,*] and Li Zhu[1,2,3,*]

[1]State Key Laboratory of Rice Biology and Breeding, China National Rice Research Institute, Hangzhou 310006, China

[2]Yazhouwan National Laboratory, Sanya 572024, China

[3]National Nanfan Research Institute (Sanya), Chinese Academy of Agricultural Sciences, Sanya 572024, China

[4]College of Life Sciences, Dezhou University, Dezhou 253023, China

[5]Shenzhen Branch, Guangdong Laboratory of Lingnan Modern Agriculture, Genome Analysis Laboratory of the Ministry of Agriculture and Rural Affairs, Agricultural Genomics Institute at Shenzhen, Chinese Academy of Agricultural Sciences, Shenzhen 518120, China

[6]College of Life Sciences, Zhejiang Normal University, Jinhua 321004, China

[7]These authors contributed equally to this article.

***Correspondence: Lianguang Shang (shanglianguang@caas.cn), Qian Qian (qianqian@caas.cn), Li Zhu (zhuli05@caas.cn)**

https://doi.org/10.1016/j.xplc.2026.101714

ABSTRACT

Early postgermination growth is critical for uniform seedling emergence in direct-seeded rice; however, the underlying regulatory mechanisms remain unclear. Here, we identified *DS1*, which encodes the shikimate pathway entry enzyme DAHPS2, from a dwarf and sterile mutant (*ds1*) in 'Huazhan' (HZ). Loss of *DS1* disrupted the shikimate pathway, reduced indole-3-acetic acid (IAA) levels through the downstream tryptophan-dependent IAA biosynthesis pathway, and induced excessive jasmonic acid (JA) accumulation, resulting in severely impaired postgermination growth. Exogenous application of the auxin analog 1-naphthaleneacetic acid or the JA biosynthesis inhibitor diethyldithiocarbamic acid partially rescued the mutant phenotype. Conversely, *DS1* overexpression elevated IAA levels, reduced JA accumulation, and promoted postgermination growth, facilitating rapid seedling emergence under submergence conditions. This effect was further validated in the 'Zhongjia 3' cultivar. We demonstrate that *DS1* is transcriptionally activated by RR26, a type-B cytokinin (CK) response regulator, through direct binding to the *DS1-7 cis* element. Using prime editing, we precisely modified *DS1-7* in HZ to generate transgene-free germplasm with improved *DS1* expression and enhanced submergence tolerance. Collectively, our findings establish an RR26–*DS1* module that regulates IAA–JA homeostasis through the shikimate pathway, providing mechanistic insights into postgermination growth and valuable genetic resources for breeding direct-seeded rice cultivars.

Key words: DAHPS2, auxin, jasmonic acid, postgermination growth, direct-seeded rice

Chen D., Hou L., Qiu Z., Xu Q., Wang Q., Li M., Hao Z., Dong P., Zhang G., Hu J., Gao Z., Dong G., Ren D., Shen L., Rao Y., Li Q., Zhang Y., Zhang Q., Guo L., Shang L., Qian Q., and Zhu L. (2026). Prime editing of an RR26-responsive *cis*-element enhances *DAHPS2* expression and submergence tolerance in rice through the shikimate pathway. Plant Comm. **7**, 101714.

INTRODUCTION

With increasing labor costs, simple and efficient dry and wet direct seeding methods have become critical for modern agricultural practices. Nevertheless, dry direct seeding is often challenged by severe weed infestation (Li et al., 2023a). Wet direct seeding, although effective for weed control, is hindered by uneven seedling emergence caused by the poor submergence tolerance of current rice varieties at the germination stage (Hsu and Tung, 2015). Therefore, the development of rice germplasm capable of rapid and uniform emergence under submerged conditions is urgently needed. Rice responds to submergence

Please cite this article in press as: Chen et al., Prime editing of an RR26-responsive *cis*-element enhances *DAHPS2* expression and submergence tolerance in rice through the shikimate pathway, Plant Communications (2026), https://doi.org/10.1016/j.xplc.2026.101714

through two major strategies: quiescence and escape (Bailey-Serres et al., 2012). Quiescence, which largely depends on the *SUBMERGENCE 1* (*SUB1*) locus, involves complex hormone signaling interactions among JA, auxin, ethylene, gibberellic acid (GA), and brassinosteroids. These interactions restrict shoot elongation and conserve carbohydrate reserves until flooding subsides (Xu et al., 2006; Khalil et al., 2024).

By contrast, the escape strategy relies on rapid coleoptile and/or mesocotyl elongation during early germination (Bailey-Serres et al., 2012; Sun et al., 2018; Pucciariello, 2020). The coleoptile, a cylindrical tissue emerging before the first leaf, determines the maximum sowing depth suitable for seedling establishment (Inada et al., 2002). Under submerged conditions, rapid coleoptile elongation is essential for seedlings to reach the water surface, thereby facilitating oxygen acquisition and supporting subsequent leaf and root development (Narsai et al., 2015). This physiological process is governed by a complex regulatory network. For example, the glucosyltransferase OsUGT75A promotes coleoptile elongation by glycosylating abscisic acid (ABA) and JA, thereby reducing their bioactive levels (He et al., 2023). The ethylene-responsive transcription factors OsEIL1 and OsEIL2 further enhance this process by upregulating reactive oxygen species–scavenging genes (Qiao et al., 2024). Additionally, salicylic acid (SA) produced by OsCNL1/2 alleviates IAA-mediated germination inhibition by regulating GH3 family-dependent auxin homeostasis (Wang et al., 2024). The OsDREB1A–OsNAC3–OsGA20ox1 transcriptional module also promotes early postgermination growth by activating the GA pathway (Huang et al., 2025). Hormonal crosstalk fine-tunes coleoptile elongation through the coordinated actions of ethylene, ABA, GA, and JA. In addition, auxin—whose biosynthesis derives from tryptophan (Trp), the end product of the shikimate pathway via the TAA1/YUCCA route—plays a central role in this regulatory network (Zhao, 2012; Casanova-Sáez et al., 2021; Wang et al., 2024). However, the precise mechanisms by which auxin interacts with other hormonal pathways to regulate coleoptile elongation remain incompletely understood.

The shikimate pathway is essential for synthesizing aromatic amino acids, including phenylalanine, tyrosine, and Trp, in plants and other organisms (Herrmann and Weaver, 1999; Maeda and Dudareva, 2012). This pathway consists of seven enzymatic steps and is initiated by 3-deoxy-D-*arabino*-heptulosonate 7-phosphate synthase (DAHPS; referred to as DHS in *Arabidopsis*). DAHPS catalyzes the condensation of phosphoenolpyruvate from glycolysis and erythrose-4-phosphate from the pentose phosphate pathway to produce 3-deoxy-D-*arabino*-heptulosonate 7-phosphate and inorganic phosphate (Herrmann and Weaver, 1999; Tzin and Galili, 2010; Yokoyama et al., 2021). DAHPS enzymes are phylogenetically classified into two types (I and II), which share low sequence identity of less than 10%. Higher plants such as *Arabidopsis*, sorghum, and rice possess type II DAHPS enzymes (Gosset et al., 2001; Webby et al., 2005; Richards et al., 2006; Tohge et al., 2013). In *Arabidopsis*, the three type II isoforms (AthDHS1, AthDHS2, and AthDHS3) exhibit distinct regulatory properties. AthDHS1 requires Mn^{2+} and reducing agents, whereas AthDHS2 is subject to feedback inhibition by tyrosine and Trp. Notably, this inhibition can be reversed through interaction with either AthDHS1 or AthDHS3 (Entus et al., 2002; Yokoyama et al., 2021). In sorghum, the DAHPS enzyme encoded by *biomass yield 1* (*BY1*) influences biomass production and grain yield (Chen et al., 2020). In rice, two DAHPS enzymes, OsDAHPS1 and OsDAHPS2, have been identified (Kanna et al., 2006). Additionally, Wang et al. (2020) demonstrated that *DNRL1*, which encodes a DAHPS enzyme, plays a crucial role in leaf morphogenesis by facilitating amino acid biosynthesis. Despite these advances, the specific molecular functions and regulatory mechanisms of DAHPS enzymes in rice remain incompletely understood.

In this study, we dissected the molecular basis of postgermination growth by characterizing the dwarf and sterile *dwarf and sterility 1* (*ds1*) mutant through map-based cloning. We revealed that *DS1* encodes DAHPS2, the entry enzyme of the shikimate pathway. Loss of *DS1* caused pleiotropic defects, including severely impaired postgermination growth, extreme dwarfism, vascular and floral abnormalities, and sterility. Mechanistically, *DS1* mutation disrupted the shikimate pathway, reduced IAA levels via the downstream Trp-dependent IAA biosynthesis pathway and induced excessive JA accumulation. Conversely, overexpression of *DS1* increased IAA levels, suppressed JA accumulation, and significantly enhanced postgermination growth under both normal and submerged conditions, including combined cold and submergence stress. These effects were consistently observed across multiple rice cultivars. Furthermore, we demonstrate that *DS1* expression is positively regulated by RR26, a type-B CK response regulator that binds to the *DS1-7* promoter element to fine-tune DS1 transcription. Finally, using prime editing, we precisely modified the structure and copy number of *DS1-7* in HZ, generating transgene-free lines with elevated *DS1 expression*. Consistent with *DS1* overexpression (*DS1-OE)* lines, these edited lines exhibited enhanced postgermination growth under submergence, providing valuable genetic resources for breeding submergence-tolerant rice varieties suitable for direct-seeded cultivation.

RESULTS

Screening and phenotypic characterization of a rice mutant exhibiting abnormal postgermination growth

In modern rice cultivation, the adoption of direct seeding is increasingly important in response to rising labor costs. A key trait for the success of this practice, particularly under submerged conditions, is rapid postgermination growth, which ensures uniform seedling emergence and establishment. However, elite germplasm resources suitable for direct seeding remain limited. To identify genetic regulators controlling postgermination growth rate, we screened an ethyl methane sulfonate-induced mutant library generated from the *indica* rice cultivar HZ. Through this screen, we identified a mutant exhibiting abnormal postgermination growth velocity. After 5 days of germination, this mutant showed markedly inhibited postgermination growth compared with the wild type (WT), characterized by significantly shorter coleoptiles, first incomplete leaves, and radicles (Figures 1A, 1H, and 1I). In contrast, seed germination was not affected (Supplemental Figures 1A–1C). At the seedling stage, the mutant showed narrow leaves, increased leaf angles (Figure 1B), and inhibited elongation of both primary and lateral roots (Figure 1C and Supplemental Figure 2A). At the heading stage, the mutant was markedly shorter than the WT (Figure 1D and Supplemental Figure 2B), produced fewer tillers (Supplemental Figure 2C) and exhibited narrow, curled leaves

Please cite this article in press as: Chen et al., Prime editing of an RR26-responsive *cis*-element enhances *DAHPS2* expression and submergence tolerance in rice through the shikimate pathway, Plant Communications (2026), https://doi.org/10.1016/j.xplc.2026.101714

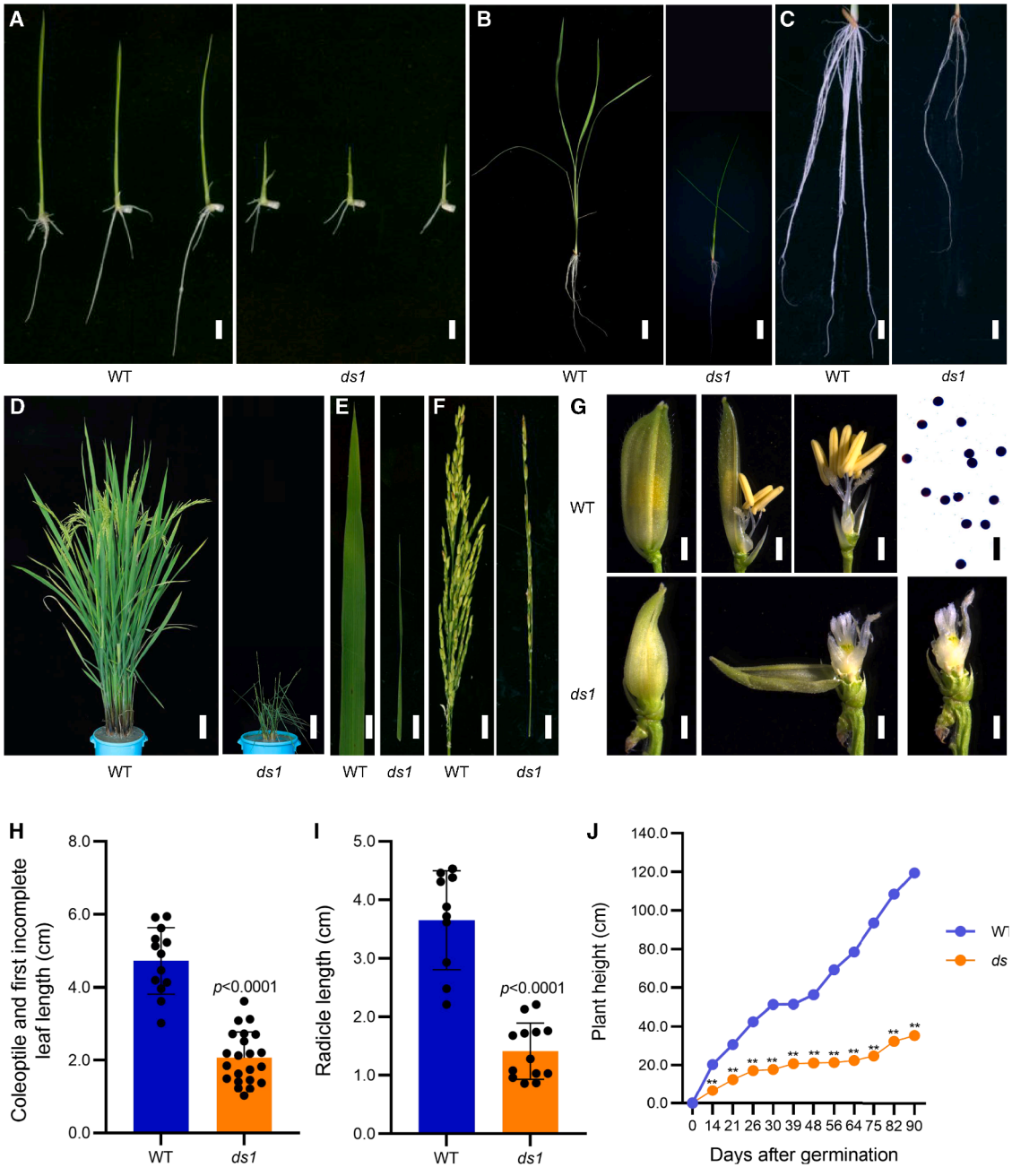

Figure 1. Phenotypes and growth dynamics of wild type (WT) and *ds1* mutant rice plants grown in the field.

(A and B) Phenotypes of WT and *ds1* mutant plants at the germination stage (**A**, 5 days old; scale bar, 1 cm) and seedling stage (**B**, 15 days old; scale bar, 3 cm).

(C) Root morphology of WT and *ds1* mutant plants at the seedling stage (scale bar, 2 cm).

(D) Phenotypes of WT and *ds1* mutant plants at the heading stage (scale bar, 10 cm).

(E and F) Leaf **(E)** and panicle **(F)** morphology of WT and *ds1* mutant plants at the heading stage (scale bar, 3 cm).

(G) Spikelet morphology and iodine staining of anthers in WT and *ds1* mutant plants at the heading stage (white scale bar, 1 mm; black scale bar, 100 μm).

(H and I) Length of the coleoptile and first incomplete leaf **(H)** and radicle **(I)** in WT and *ds1* mutant plants after 5 days of germination. Values represent means ± SD of 10 biological replicates. *P* values were determined by a two-tailed Student's *t*-test.

(J) Plant height dynamics of WT and *ds1* mutant plants during the reproductive period. Values represent means ± SD of three biological replicates. Significant differences compared with WT were determined by Student's *t*-test (**$P < 0.01$).

(Figure 1E and Supplemental Figure 2D). The angles between the flag and penultimate leaves were enlarged (Supplemental Figure 2E). In addition, panicles were severely malformed, with abnormal stigmas, absence of anthers, and complete sterility (Figures 1F and 1G). Overall, the mutant exhibited pronounced growth retardation throughout its entire life cycle (Figure 1J). Based on these pleiotropic phenotypes, the mutant was designated *dwarf and sterility 1* (*ds1*).

Please cite this article in press as: Chen et al., Prime editing of an RR26-responsive *cis*-element enhances *DAHPS2* expression and submergence tolerance in rice through the shikimate pathway, Plant Communications (2026), https://doi.org/10.1016/j.xplc.2026.101714

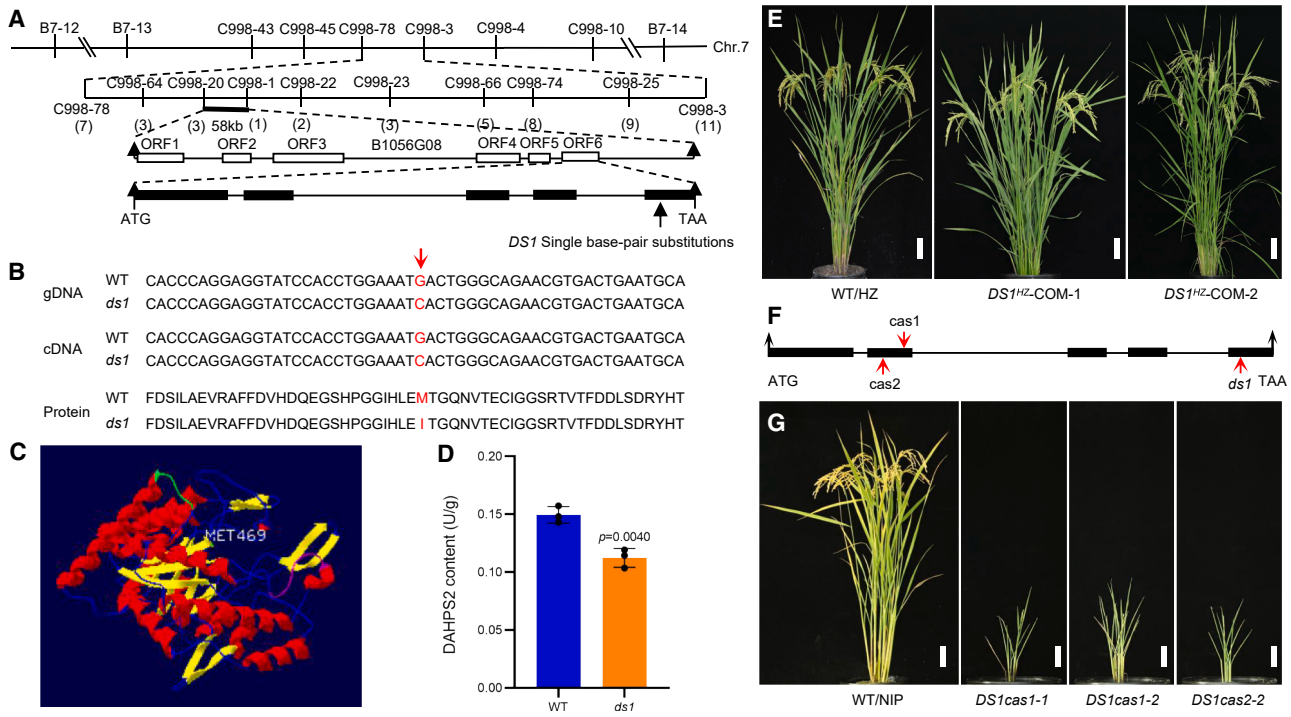

Figure 2. Map-based cloning, DAHPS2 enzyme activity, and genetic validation of *DS1*.

(A) The *ds1* locus was initially mapped to chromosome 7 (Chr. 7) and subsequently fine-mapped to a 58-kb physical interval using the indicated molecular markers.

(B) Mutation sites in *ds1* at the genomic DNA and protein levels.

(C) Predicted monomeric DS1 protein structure generated using SWISS-MODEL. Green indicates the cas1 target site, purple indicates the cas2 target site, and Met469 denotes the *ds1* mutation site.

(D) DAHPS2 enzyme activity in WT and *ds1* plants. Values represent means ± SD of three biological replicates. *P* values were determined by a two-tailed Student's *t*-test.

(E) Genetic complementation of the rice *ds1* mutant. From left to right: WT and two independent *DS1* complementation lines at maturity (scale bar, 10 cm).

(F) Schematic representation of the different mutation sites introduced into *DS1*.

(G) Phenotypes of mature mutant plants harboring two distinct *DS1*-targeted Cas9/sgRNA constructs (scale bar, 10 cm).

Microscopic examination revealed that *ds1* leaves at the seedling stage possessed only one large vein on each side and lacked small veins, whereas WT leaves contained three large veins and multiple small veins (Supplemental Figure 3A). At the heading stage, *ds1* leaves exhibited fewer large and small veins per side compared with the WT (Supplemental Figure 3B), accounting for the narrow-leaf phenotype. In the top1 and top2 regions of the *ds1* leaf joints, an increased number of sclerenchyma cells was observed on both the abaxial and adaxial sides relative to the WT, whereas the top3 region showed no obvious difference between the two genotypes (Supplemental Figures 3C–3E). The increased sclerenchyma accumulation on the adaxial side likely contributed to the greater leaf angles observed in *ds1*. In addition, ligules in *ds1* were significantly smaller than those in the WT (Supplemental Figures 3C–3E). Panicle development was also severely disrupted in *ds1*, with flowers lacking stamens and anthers and containing only a hardened pistil, resulting in sterility (Supplemental Figures 3F and 3G).

DS1 encodes DAHPS2, the entry enzyme of the shikimate pathway

To fine-map the *DS1* gene, a mapping population was created by crossing the *japonica* rice cultivar 'Wuyungeng 7' (WYG7) as the male parent with heterozygous *ds1* mutant plants as the female parent. All F_1 hybrids displayed normal phenotypes. *ds1 mutant individuals were subsequently selected* from the F_2 population generated by selfing F_1 plants for genetic mapping.

Using 21 *ds1* mutant plants from the WYG7 × heterozygous *ds1* cross, *DS1* was initially mapped to the distal region of the long arm of chromosome 7. By expanding the F_2 population to 16 300 individuals and developing new simple sequence repeat and sequence-tagged site markers (Supplemental Table 1), the mapping interval was narrowed to a 58 kb region on chromosome 7 (Figure 2A). Sequencing of six candidate open reading frames within this interval identified a single nucleotide substitution (G1407C) in the fifth exon of *LOC_Os07g42960*, which results in a missense mutation (M469I) (Figures 2B–2E). This gene is predicted to encode DAHPS2, the entry enzyme of the shikimate pathway that catalyzes the condensation of phosphoenolpyruvate and erythrose-4-phosphate to form 3-deoxy-D-*arabino*-heptulosonate 7-phosphate, a key step in aromatic amino acid biosynthesis (Supplemental Figure 4A) (Maeda and Dudareva, 2012). Although the mutation did not alter the overall protein structure of DAHPS2 (Supplemental Figure 4B), its enzymatic activity was significantly reduced in the *ds1* mutant compared with the WT (Figure 2G).

Please cite this article in press as: Chen et al., Prime editing of an RR26-responsive *cis*-element enhances *DAHPS2* expression and submergence tolerance in rice through the shikimate pathway, Plant Communications (2026), https://doi.org/10.1016/j.xplc.2026.101714

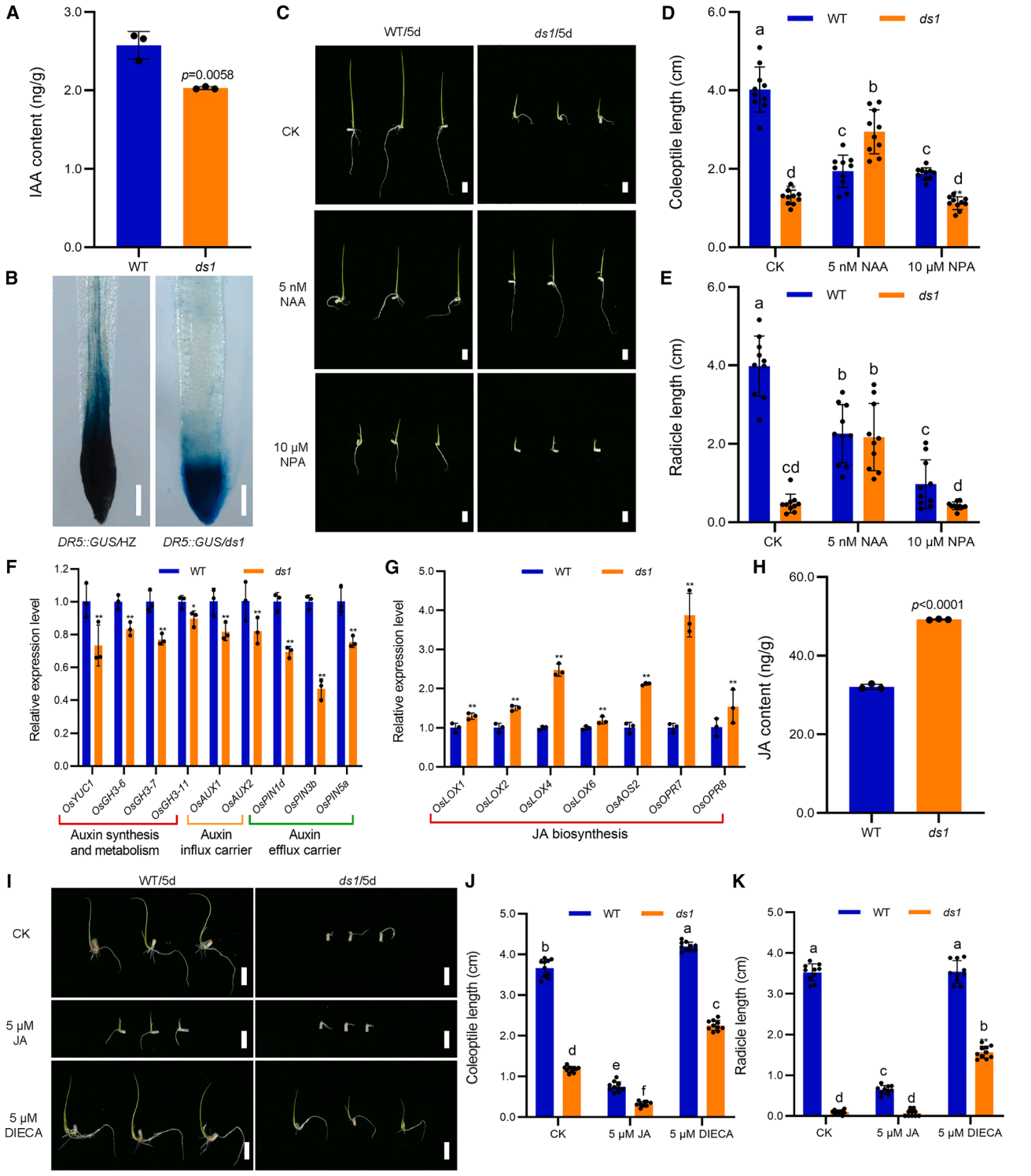

Figure 3. Regulation of postgermination growth by auxin and JA in WT and *ds1* mutants.

(A) IAA content in the coleoptile and first incomplete leaf of WT and *ds1* mutant plants after 5 days of germination. Values represent means ± SD of three biological replicates. *P* values were determined by a two-tailed Student's *t*-test.

(B) GUS staining in 8-cm root tips of *DR5::GUS*/HZ and *DR5::GUS*/*ds1* transgene-positive plants (scale bar, 200 μm).

(C) Phenotypes of WT and *ds1* seeds after a 5-day treatment with 5 nM NAA or 10 μM NPA. From top to bottom: dehulled seeds under control conditions without exogenous hormones, 5 nM NAA, or 10 μM NPA (scale bar, 1 cm).

(legend continued on next page)

Please cite this article in press as: Chen et al., Prime editing of an RR26-responsive *cis*-element enhances *DAHPS2* expression and submergence tolerance in rice through the shikimate pathway, Plant Communications (2026), https://doi.org/10.1016/j.xplc.2026.101714

To confirm that *LOC_Os07g42960* corresponds to *DS1*, we performed a complementation assay by introducing the full-length *DS1* genomic sequence from HZ into the *ds1* heterozygous background. Sequencing and phenotypic analyses confirmed that expression of the wild-type *DS1 gene fully rescued* the *ds1* mutant phenotypes (Figure 2H and Supplemental Figures 4E and 4F). Additionally, we designed two CRISPR–Cas9 knockout target sites (cas1 and cas2) in the 'Nipponbare' (NIP) background (Figure 2I). The resulting knockout lines carrying diverse mutation patterns (Supplemental Figures 4C and 4D) exhibited disrupted DAHPS2 protein structures (Supplemental Figure 4B) and phenocopied the *ds1* mutant (Figure 2J and Supplemental Figures 4G and 4H). Together, these results demonstrate that mutation of the *DS1* gene is responsible for the *ds1* mutant phenotype.

DS1 regulates postgermination growth by modulating IAA biosynthesis and JA accumulation

Expression analysis revealed that *DS1* is transcribed in multiple tissues, with the highest expression detected in root tips (Supplemental Figures 5A and 5B). Sequence alignment further showed that DS1 is highly conserved across different species, suggesting an evolutionarily conserved role in rice growth and development (Supplemental Figures 5C and 5D).

Because Trp, a downstream product of the shikimate pathway, serves as a direct precursor for the Trp-dependent IAA biosynthesis pathway (Supplemental Figure 6A) (Zhao, 2010; Maeda and Dudareva, 2012), we hypothesized that IAA homeostasis might be altered in the *ds1* mutant. Consistent with this hypothesis, Trp and IAA contents in the coleoptile and first incomplete leaf of *ds1 seedlings at* 5 days of germination were significantly lower than those in the WT (Supplemental Figure 6B; Figure 3A). In addition, β-glucuronidase (GUS) staining further confirmed reduced auxin accumulation in *ds1* (Figure 3B).

To investigate whether exogenous auxin could rescue the *ds1* phenotype, WT and *ds1* seedlings were treated with 20 μM IAA. Root elongation in *ds1* increased by 5.96% compared with the untreated mutant but remained significantly shorter than that of the WT (Supplemental Figures 7A and 7B), indicating only partial phenotypic rescue by IAA supplementation. When treated with yucasin, an inhibitor of auxin biosynthesis mediated by YUCCA enzymes (Nishimura et al., 2014), root elongation was suppressed in both genotypes. Notably, this inhibitory effect was weaker in *ds1*, with an 8.12% reduction compared with a 15.04% reduction in the WT (Supplemental Figures 7C and 7D), further supporting the conclusion that the *DS1* mutation compromises endogenous IAA biosynthesis.

To distinguish whether the growth defects in *ds1* result from impaired auxin biosynthesis or defective auxin transport, we treated WT and *ds1* seedlings with 1-naphthaleneacetic acid (NAA), an IAA analog that enters cells via passive diffusion and therefore bypasses polar auxin transport (Yamamoto and Yamamoto, 1998; Tan et al., 2007). Treatment with 5 nM NAA significantly rescued the *ds1* mutant phenotype (Figures 3C–3E), indicating that impaired IAA biosynthesis, rather than defective transport, underlies the observed growth defects. Conversely, treatment with 10 μM 1-naphthylphthalamic acid (NPA), an inhibitor of auxin efflux (Huang et al., 2017), further exacerbated the radicle growth defects in *ds1* (Figures 3C–3E). Together, these results demonstrate that DS1, as the entry enzyme of the shikimate pathway, acts as a key upstream regulator of IAA homeostasis in rice by maintaining adequate IAA biosynthesis and enabling proper downstream developmental responses.

To further investigate the broader impact of *DS1* on rice growth regulation, we performed RNA sequencing analysis on both shoot and root tissues of 7-day-old WT and *ds1* seedlings after germination. Gene ontology enrichment analysis revealed that *DS1* is closely linked to plant hormone signal transduction pathways (Supplemental Figure 8A). Based on this observation, we examined whether DS1 also influences hormonal pathways beyond auxin. Consistent with earlier results, genes involved in auxin biosynthesis, metabolism, and transport were significantly downregulated in *ds1* (Supplemental Figure 8B and Figure 3F), whereas genes related to JA biosynthesis were upregulated (Supplemental Figure 8B and Figure 3G). Because JA is known to inhibit plant growth (Dathe et al., 1981; Chen et al., 2011), we hypothesized that elevated JA levels contribute to the impaired postgermination growth observed in *ds1*. To test this hypothesis, we measured hormone levels in the coleoptile and first incomplete leaf of WT and ds1 seedlings 5 days after germination and found that JA levels were significantly higher in the mutant (Figure 3H). Exogenous application of JA severely inhibited WT growth, mimicking the *ds1* phenotype (Figures 3I–3K). Conversely, treatment with the JA biosynthesis inhibitor DIECA (Farmer et al., 1994) restored postgermination growth in *ds1* to WT levels (Figures 3I–3K). These findings indicate that excessive JA accumulation partially contributes to the postgermination growth defects of the *ds1* mutant and in conjunction with impaired auxin biosynthesis, underlies the growth-regulatory function of DS1.

(D and E) Coleoptile **(D)** and radicle **(E)** lengths of WT and *ds1* after 5 days of NAA or NPA treatment. Ten seeds were analyzed per treatment. Significant differences compared with WT were determined using Student's *t*-test (**$P < 0.01$). Different lowercase letters above the bars indicate significant differences determined by two-way ANOVA followed by Tukey's post hoc test ($P < 0.05$).
(F and G) Quantitative RT–PCR analysis of auxin-related **(F)** and JA-related **(G)** gene expression in WT and *ds1* mutant plants after 7 days of germination. Values represent means ± SD of three biological replicates. Significant differences compared with WT were determined using Student's *t*-test (**$P < 0.01$).
(H) JA content in the coleoptile and first incomplete leaf of WT and *ds1* mutant plants after 5 days of germination. Values represent means ± SD of three biological replicates. *P* values were determined by a two-tailed Student's *t*-test.
(I) Phenotypes of WT and *ds1* mutant seeds treated with 5 μM JA or 5 μM DIECA for 5 days. From top to bottom: dehulled seeds under control conditions without exogenous hormones, 5 μM JA, and 5 μM DIECA (scale bar, 1 cm).
(J and K) Coleoptile **(J)** and radicle **(K)** lengths of WT and *ds1* mutant seeds after 5 days of JA or DIECA treatment. Ten seeds were analyzed per treatment. Different lowercase letters above the bars indicate significant differences determined by two-way ANOVA followed by Tukey's post hoc test ($P < 0.05$).

Please cite this article in press as: Chen et al., Prime editing of an RR26-responsive *cis*-element enhances *DAHPS2* expression and submergence tolerance in rice through the shikimate pathway, Plant Communications (2026), https://doi.org/10.1016/j.xplc.2026.101714

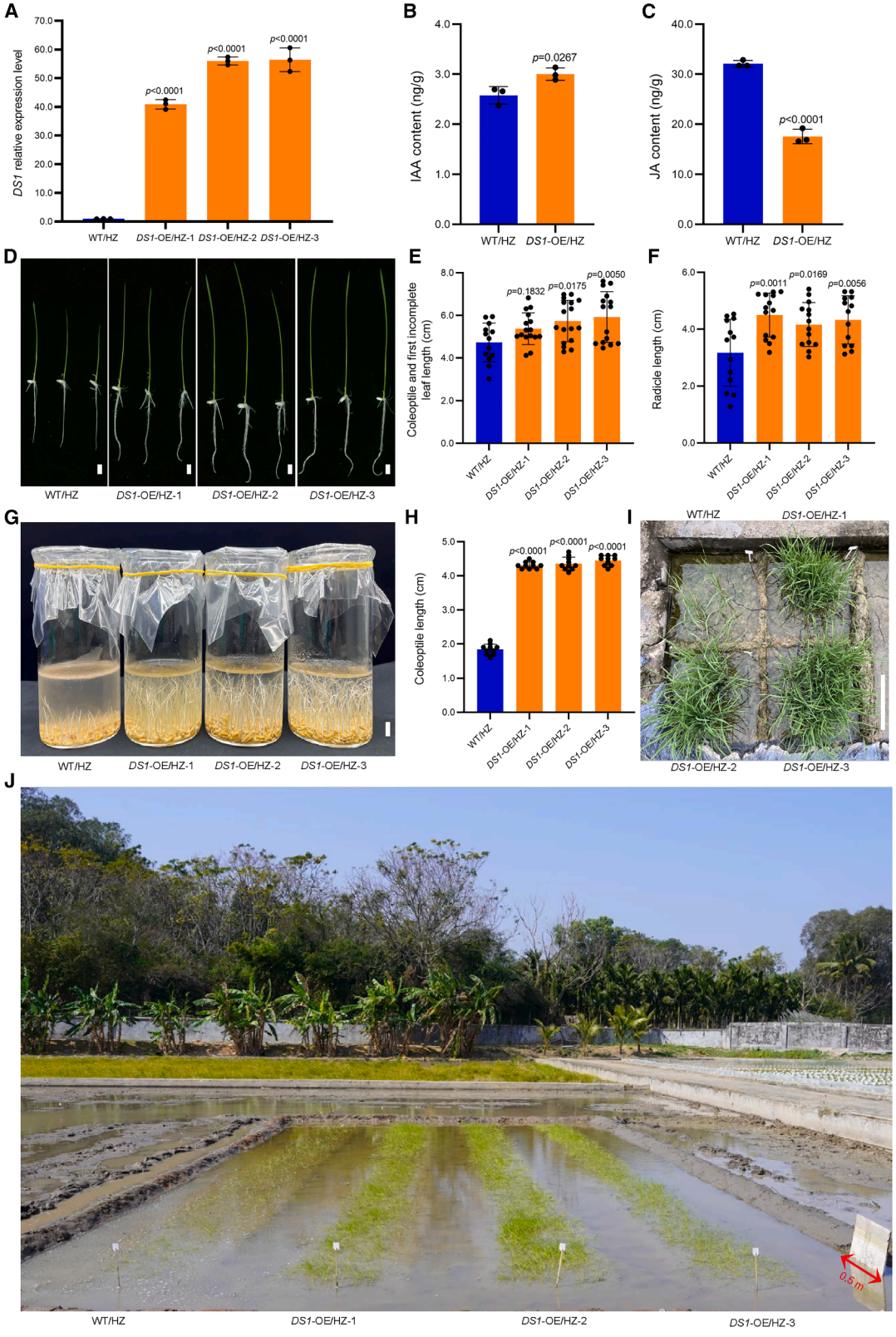

Figure 4. *DS1* overexpression significantly enhances submergence tolerance.

(A) Relative DS1 transcript levels in the coleoptile and first incomplete leaf of WT/HZ and three independent *DS1*-OE/HZ lines after 5 days of germination. Values represent means ± SD of three biological replicates. *P* values were determined by one-way ANOVA.

(legend continued on next page)

Please cite this article in press as: Chen et al., Prime editing of an RR26-responsive *cis*-element enhances *DAHPS2* expression and submergence tolerance in rice through the shikimate pathway, Plant Communications (2026), https://doi.org/10.1016/j.xplc.2026.101714

Overexpression of *DS1* significantly enhances rice postgermination growth

Previous experiments showed no significant difference in germination rates between *ds1* and the WT (Supplemental Figures 1A–1C). However, postgermination growth was markedly inhibited in *ds1* compared with the WT (Figures 1A, 1H, and 1I), primarily due to reduced IAA levels and elevated JA levels (Figures 3A and 3H). These findings prompted us to investigate whether *DS1* overexpression could enhance postgermination growth. To this end, we generated three *DS1*-OE lines in the HZ background (Figure 4A) and measured their IAA and JA levels. Compared with WT/HZ, *DS1*-OE/HZ lines exhibited elevated IAA levels (Figure 4B) and markedly reduced JA levels (Figure 4C). Consistent with these hormonal changes, *DS1*-OE/HZ seedlings exhibited significantly longer coleoptiles, first incomplete leaves, and radicles relative to WT/HZ 5 days after germination (Figures 4D–4F).

Wet direct seeding is often hindered by uneven seedling emergence due to the poor submergence tolerance of current rice varieties during germination (Hsu and Tung, 2015). Under submerged conditions, seeds may fail to rapidly reach the water surface, leading to mold growth and seedling death. We therefore hypothesized that the accelerated postgermination growth observed in *DS1*-OE/HZ lines would promote rapid coleoptile elongation and facilitate more efficient escape from submergence. Consistent with this hypothesis, under laboratory conditions with a 5 cm water depth, *DS1*-OE/HZ lines developed significantly longer coleoptiles than WT/HZ, indicating enhanced submergence tolerance (Figures 4G and 4H). To further assess whether this effect is conserved across genetic backgrounds, we generated three *DS1*-OE lines in the *japonica* cultivar 'Zhongjia 3' (*DS1*-OE/ZJ3). All *DS1*-OE/ZJ3 *lines similarly exhibited superior submergence tolerance compared with their corresponding WT controls* (Supplemental Figures 9A–9C).

Given that direct-seeded rice, particularly in spring, often faces low-temperature stress that impairs germination and early seedling establishment, we further evaluated *DS1*-OE/HZ lines under combined cold and submergence conditions (15°C, 14/10 h day/night cycle, 5 cm water depth). Under these conditions, *DS1*-OE/HZ lines consistently maintained significantly longer coleoptiles than WT/HZ (Supplemental Figures 10A–10D).

Collectively, these results demonstrate that *DS1* overexpression enhances seedling emergence rate and uniformity by accelerating postgermination growth, thereby enabling rapid escape from submerged conditions. This advantage is maintained even under low-temperature stress and is associated with elevated IAA levels and an optimized IAA–JA balance in *DS1* overexpression lines.

To assess the performance of this germplasm under complex and variable environments, we conducted field trials. In summer field experiments under normal temperatures in Fuyang, *DS1*-OE/HZ lines exhibited faster elongation and more uniform seedling emergence under submerged conditions than WT/HZ (Figure 4I). Consistently, large-scale winter field trials in Hainan confirmed that the *DS1*-OE/HZ lines consistently outperformed the WT (Figure 4J and Supplemental Figures 11A–11I). Notably, during the direct-seeding period in Hainan, ambient temperatures remained near 15°C for nearly half of the time (Supplemental Figure 11J). Taken together, our findings indicate that DS1-mediated acceleration of postgermination growth significantly enhances rice adaptation to direct-seeding environments.

The RR26 transcription factor enhances *DS1* expression

To elucidate the regulatory mechanism underlying *DS1* expression, we sought to identify its upstream transcriptional regulators. We first analyzed the *DS1* promoter using the PlantRegMap database (https://plantregmap.gao-lab.org/) to predict potential transcription factor binding sites. Candidate regulators were then screened using firefly luciferase (LUC) reporter assays, leading to the identification of RR26 (LOC_Os01g67770), a type-B CK response regulator (Li et al., 2024) (Figures 5A and 5B). This interaction was further validated by LUC assays in tobacco epidermal cells, which showed a strong LUC signal, indicating that RR26 activates *DS1* transcription (Figure 5C). To determine whether RR26 directly binds to the *DS1 promoter*, we performed yeast one-hybrid (Y1H) assays to test its interaction with the predicted *DS1* cis element *DS1-7*, located at −242 to −232 bp relative to the transcription start site. Although the full-length *DS1* promoter exhibited self-activation, this effect was eliminated when *DS1-7* was used alone. Under these conditions, RR26 binding was confirmed by the appearance of blue colonies (Figures 5D and 5E). Electrophoretic mobility shift assays (EMSA) further verified the direct binding of RR26 to *DS1-7 in vitro* (Figure 5F). Subcellular localization analysis showed that RR26 localizes to the nucleus (Supplemental Figure 12), and sequence alignment revealed high conservation of RR26 across plant species, suggesting an evolutionarily conserved function in growth regulation (Supplemental Figures 13A and 13B).

Having established the molecular interaction between RR26 and DS1, we next sought genetic evidence to confirm that RR26 acts as a positive regulator of *DS1 in planta*. Knockout of *RR26* (*rr26*) resulted in postgermination growth defects that closely

(B and C) IAA **(B)** and JA **(C)** contents in the coleoptile and first incomplete leaf of WT/HZ and *DS1*-OE/HZ lines after 5 days of germination. Values represent means ± SD of three biological replicates. *P* values were determined by a two-tailed Student's *t*-test.
(D) Phenotypes of WT/HZ and *DS1*-OE/HZ lines after 5 days of germination on 1/2 MS medium (scale bar, 1 cm).
(E and F) Coleoptile and first incomplete leaf lengths **(E)** and radicle length **(F)** of WT/HZ and *DS1*-OE/HZ lines after 5 days of germination on half-strength MS (1/2 MS) medium. Data represent means ± SD from 20 seeds per genotype. *P* values were determined by one-way ANOVA.
(G) Phenotypes of WT/HZ and *DS1*-OE/HZ lines after 10 days of germination under 5-cm submergence (scale bar, 1 cm).
(H) Coleoptile length of WT/HZ and *DS1*-OE/HZ lines after 10 days of germination under 5-cm submergence. Data represent means ± SD from 300 seeds per genotype. *P* values were determined by one-way ANOVA.
(I) Phenotypes of WT/HZ and *DS1*-OE/HZ lines after 25 days of dry sowing followed by continuous 5-cm submergence treatment in the field in Fuyang, Zhejiang, China (scale bar, 0.5 m).
(J) Phenotypes of WT/HZ and *DS1*-OE/HZ lines after 23 days of dry sowing followed by continuous 5-cm submergence treatment in the field in Lingshui, Hainan, China. The length of the white baffle is 0.5 m.

Please cite this article in press as: Chen et al., Prime editing of an RR26-responsive *cis*-element enhances *DAHPS2* expression and submergence tolerance in rice through the shikimate pathway, Plant Communications (2026), https://doi.org/10.1016/j.xplc.2026.101714

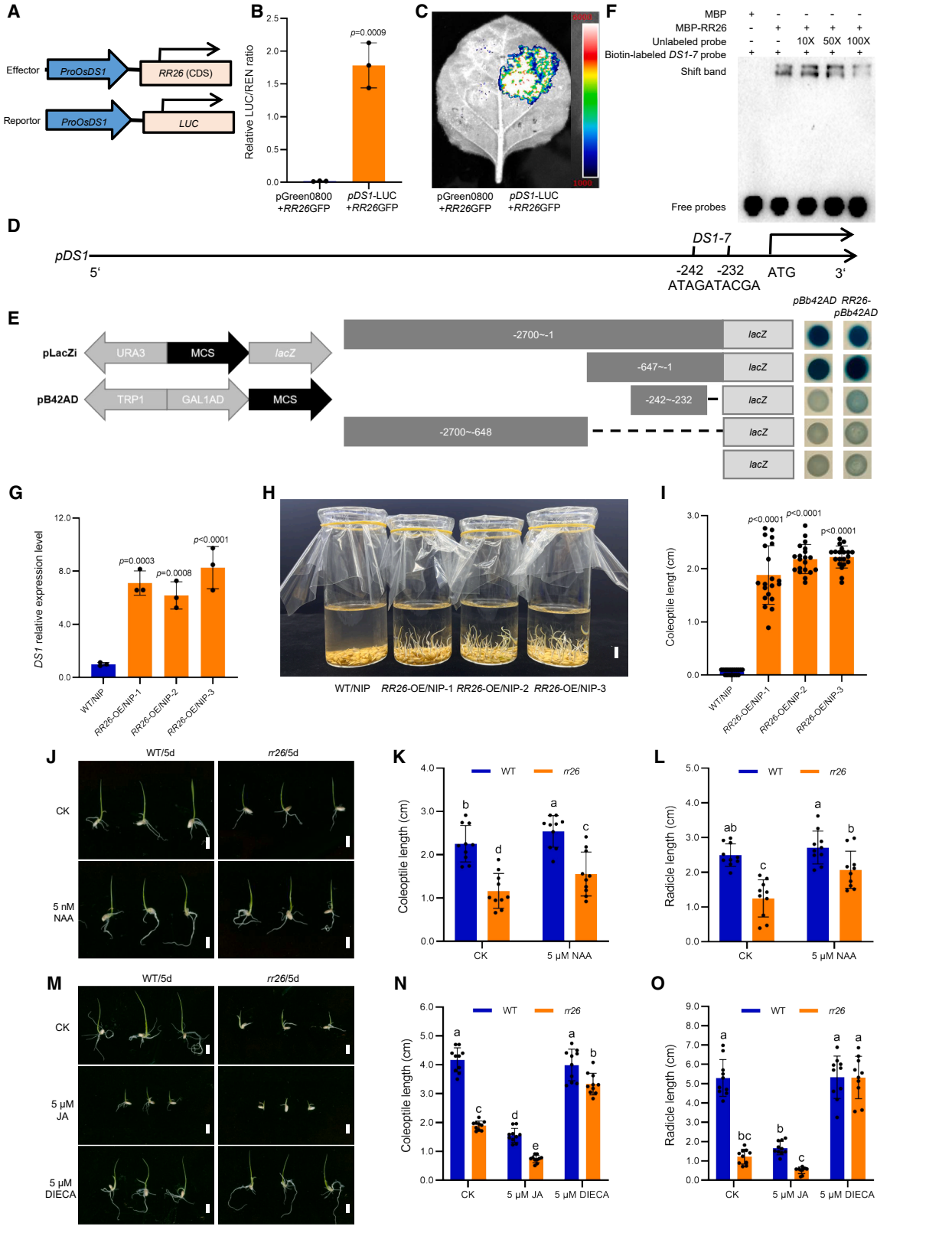

Figure 5. RR26 activates *DS1* expression to balance IAA–JA antagonism.

(A and B) Luciferase transient transactivation assays in rice protoplasts. Constructs used in the transient expression assays are shown in **(A)**. RR26 significantly activates *DS1* transcription **(B)**. Values represent means ± SD of three biological replicates. *P* values were determined by a two-tailed Student's *t*-test.

(legend continued on next page)

Please cite this article in press as: Chen et al., Prime editing of an RR26-responsive *cis*-element enhances *DAHPS2* expression and submergence tolerance in rice through the shikimate pathway, Plant Communications (2026), https://doi.org/10.1016/j.xplc.2026.101714

phenocopied the *ds1* mutant (Supplemental Figures 14A–14D). In contrast, overexpression of *RR26* in the NIP background (*RR26*-OE/NIP) resulted in a marked increase in DS1 transcript abundance and enhanced submergence tolerance, closely resembling the *DS1* overexpression phenotype (Figures 5G–5I).

Further physiological characterization revealed that RR26 also participates in hormonal regulation during early seedling development. The inhibited postgermination growth of *rr26* seedlings was partially rescued by treatment with NAA (Figures 5J–5L), indicating that RR26 contributes to auxin regulation. Moreover, exogenous JA treatment significantly inhibited WT growth, mimicking the *rr26* phenotype, whereas treatment with DIECA alleviated this inhibition (Figures 5M–5O). These results suggest that RR26 also functions in JA homeostasis.

Together, these results demonstrate that RR26 directly binds to the *DS1* promoter at the *DS1-7* element to activate *DS1* expression, thereby functioning as a key upstream positive regulator of postgermination growth.

Precision editing of *DS1* improves submergence tolerance in direct-seeded rice

Our findings indicate that elevated *DS1* expression improves submergence tolerance in direct-seeded rice by promoting postgermination growth. We therefore asked whether natural germplasm resources harbor elite alleles associated with increased *DS1* expression. To address this, we analyzed SNP variation within a 2.5 kb region upstream of the *DS1* coding sequence across a rice micro-core collection, as previously described (Shang et al., 2022). Four haplotypes (Hap1–Hap4) were identified, showing clear divergence between *indica* and *japonica* cultivars (Supplemental Figure 15A). However, transcriptome data from Shang et al. (2022) revealed no significant differences in DS1 transcript abundance among these haplotypes (Supplemental Figure 15B). Consistently, promoter activity assays showed only minimal differences between *indica*- and *japonica*-type promoters (Supplemental Figure 15C). These results indicate that natural promoter polymorphisms within the surveyed germplasm have limited effects on *DS1* expression.

Given that RR26 functions as a transcriptional activator of *DS1*, we next investigated how it regulates *DS1* expression. LUC assays defined the core *DS1* promoter region as −232 to −1 bp relative to the transcription start site (Figure 6A). Notably, increasing the copy number of the RR26 binding motif *DS1-7* led to a linear increase in the LUC/*Renilla luciferase* (REN) ratio (Figure 6B), supporting the notion that RR26 positively regulates DS1 transcription in a dosage-dependent manner.

Based on these findings, we hypothesized that increasing the number of RR26 binding sites in the *DS1* promoter could enhance *DS1* expression. We therefore selected the *DS1-7* motif as a target for genome editing and employed the ePE2 prime-editing system (Li et al., 2023b; Zou et al., 2025) to integrate three tandem copies of *DS1-7* into the native *DS1* promoter. The resulting edited lines showed four distinct integration patterns (Figure 6C). Despite this variability, RT–qPCR analysis confirmed significantly elevated DS1 transcript levels in all edited lines (Figure 6D). Following segregation and removal of exogenous editing components, submergence assays showed that the edited lines developed markedly longer coleoptiles than the WT, reflecting enhanced submergence tolerance (Figures 6E and 6F). Importantly, no obvious developmental abnormalities were observed at later growth stages (Supplemental Figures 16A–16G).

Collectively, these results elucidate the regulatory mechanism by which RR26 activates *DS1* transcription and demonstrate that targeted promoter editing represents a feasible and promising strategy for generating transgene-free rice germplasm with improved submergence tolerance for direct-seeded cultivation.

DISCUSSION

This study demonstrates that *DS1*, which encodes the entry enzyme of the shikimate pathway, plays a central role in regulating rice postgermination growth by maintaining hormonal homeostasis and enhancing submergence tolerance (Figure 7).

Mutations at critical sites in *DS1* cause pleiotropic phenotypes by disrupting DAHPS2 catalytic activity

To confirm that the severe *ds1* phenotype is indeed caused by mutation of the *DS1* gene, we generated two CRISPR–Cas9 knockout lines targeting *DS1* (cas1 and cas2) (Figure 2I). Among the knockout lines targeting cas1, four displayed phenotypes resembling *ds1* (Figure 2J and Supplemental Figure 4C).

(C) Luciferase imaging assay in tobacco leaves showing RR26-mediated activation of*DS1* transcription.
(D and E) Y1H assays confirming RR26 binding to the *DS1-7* promoter element.
(F) EMSA demonstrating RR26 binding to the biotin-labeled *DS1-7* DNA probe.
(G) Relative DS1 transcript levels in the coleoptile and first incomplete leaf of WT/NIP and *RR26*-OE/NIP lines after 5 days of germination. Values represent means ± SD of three biological replicates. *P* values were determined by one-way ANOVA.
(H) Phenotypes of WT/NIP and three independent *RR26*-OE/NIP lines after 8 days of germination under 5 cm submergence (scale bar, 1 cm).
(I) Coleoptile lengths of WT/NIP and three independent *RR26*-OE/NIP lines after 8 days of germination under 5-cm submergence. *P* values were determined by one-way ANOVA.
(J) Phenotypes of WT and *rr26* mutant seeds after 5 days of NAA treatment. From top to bottom: dehulled seeds of WT and *rr26* under control conditions (no exogenous hormones) and 5 nM NAA (scale bar, 1 cm).
(K and L) Coleoptile **(K)** and radicle **(L)** lengths of WT and *rr26* mutant seeds after 5 days of NAA treatment. Ten seeds were assessed per treatment. Different lowercase letters above the bars indicate significant differences determined by two-way ANOVA followed by Tukey's post hoc test ($P < 0.05$).
(M) Phenotypes of WT and *rr26* mutant seeds after 5 days of JA or DIECA treatment. From top to bottom: dehulled seeds of WT and *rr26* under control conditions (no exogenous hormones), 5 μM JA, and 5 μM DIECA (scale bar, 1 cm).
(N and O) Coleoptile **(N)** and radicle **(O)** lengths of WT and *rr26* mutant seeds after 5 days of JA or DIECA treatment. Ten seeds were analyzed per treatment. Different lowercase letters above the bars indicate significant differences determined by two-way ANOVA followed by Tukey's post hoc test ($P < 0.05$). Significant differences compared with WT were determined using Student's *t*-test (**$P < 0.01$).

Please cite this article in press as: Chen et al., Prime editing of an RR26-responsive *cis*-element enhances *DAHPS2* expression and submergence tolerance in rice through the shikimate pathway, Plant Communications (2026), https://doi.org/10.1016/j.xplc.2026.101714

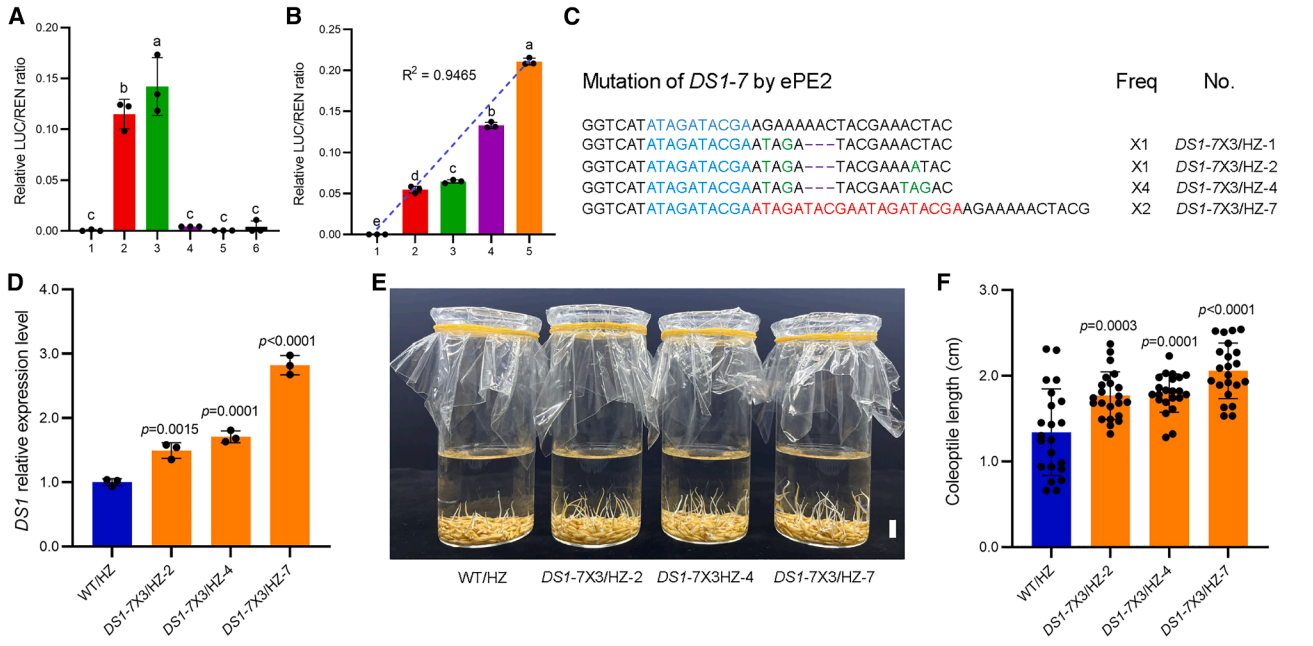

Figure 6. Development of novel direct-seeded rice germplasm via *DS1* modification to enhance submergence tolerance.

(A) Identification of the *DS1* core promoter region (−232 to −1 bp) using LUC assays. Constructs assayed (1–6) were pGreen0800+*RR26*GFP (negative control), *pDS1-232*+*RR26*GFP, *pDS1-647*+*RR26*GFP, *pDS1-7*+*RR26*GFP, *pDS1-7*X2+*RR26*GFP, and *pDS1-7*X3+*RR26*GFP.

(B) Dose-dependent activation of the *DS1* promoter by RR26. LUC/REN ratios increased with increasing copy number of the RR26-binding motif *DS1-7*. Constructs assayed (1–5) were pGreen0800+*RR26*GFP (negative control), *pDS1-232*+*RR26*GFP, *pDS1-7*+232+*RR26*GFP, *pDS1-7*X2+232+*RR26*GFP, and *pDS1-7*X3+232+*RR26*GFP.

Data in **(A)** and **(B)** represent means ± SD of three biological replicates. Different lowercase letters above the bars indicate significant differences determined by one-way ANOVA followed by Tukey's post hoc test ($P < 0.05$).

(C) Schematic of ePE2-mediated editing of the *DS1-7* element. The target sequence is highlighted in blue, substituted nucleotides are shown in green, deleted nucleotides are indicated by purple dashes, and inserted nucleotides are shown in red.

(D) Relative DS1 transcript levels in WT/HZ and three independent *DS1-7*X3 edited lines after removal of exogenous components. Values represent means ± SD of three biological replicates. *P* values were determined by one-way ANOVA.

(E) Phenotypes of WT/HZ and three *DS1-7*X3 modified lines after 8 days of germination under 5-cm submergence (scale bar, 1 cm).

(F) Coleoptile lengths of WT/HZ and three *DS1-7*X3 edited lines after 8 days of germination under 5-cm water submergence. Data represent means ± SD from 100 seeds per genotype. *P* values were determined by one-way ANOVA.

Interestingly, we also identified one line with a normal phenotype (*DS1cas1-N*) (Supplemental Figure 17B). This line carried a three-base deletion (CGA) at the target site (Supplemental Figure 17A), resulting in the loss of a serine residue and a glutamate-to-arginine substitution. Protein structure modeling predicted no substantial conformational alterations (Supplemental Figure 17C), and enzymatic activity assays revealed a slight increase in DAHPS2 activity (Supplemental Figure 17D). Consistently, agronomic trait analysis showed no significant differences between *DS1cas1-N* and the WT (Supplemental Figure 17E). A similar observation was reported for the *dnrl1* mutant by Wang et al. (2020), in which a single nucleotide substitution (T1127A) in the fourth exon caused a leucine-to-histidine substitution at position 376 (L376H) without affecting protein structure or enzymatic activity (Supplemental Figure 17D).

By contrast, the *ds1* mutant carries a SNP (G1407C) in the fifth exon, resulting in a methionine-to-isoleucine substitution at position 469 (M469I) (Figures 2C–2E). Although structural modeling predicted only minor conformational changes (Figure 2F; Supplemental Figure 4B), DAHPS2 enzymatic activity was markedly reduced (Figure 2G), leading to the severe *ds1* phenotype (Figures 1A–1G). These findings suggest that the *ds1* mutation disrupts a critical catalytic region of DS1, whereas minor alterations in non-essential regions have limited functional consequences. Overall, the fifth exon of *DS1* appears to be essential for its catalytic activity. Further studies using protein crystallography and site-directed mutagenesis will be required to precisely define the residues critical for DAHPS2 activity.

DS1 may act as a shikimate pathway gatekeeper that bridges crosstalk among multiple hormone signaling pathways

Our results demonstrate that *DS1*, encoding a DAHPS enzyme, is essential for coordinating hormonal balance during rice postgermination growth. As the entry point of the shikimate pathway, loss of DS1 function disrupts IAA biosynthesis, as evidenced by the significant rescue of *ds1* defects following NAA application (Figures 3C–3E). Concurrently, *ds1* mutants accumulated higher levels of JA, likely as an indirect consequence of impaired shikimate pathway flux. Inhibition of JA biosynthesis partially restored postgermination growth in *ds1* (Figures 3I–3K), revealing a critical DS1-dependent antagonistic relationship between IAA and JA.

This antagonism aligns with established hormonal dynamics in submerged rice seedlings. The quiescence strategy, typified by

Please cite this article in press as: Chen et al., Prime editing of an RR26-responsive *cis*-element enhances *DAHPS2* expression and submergence tolerance in rice through the shikimate pathway, Plant Communications (2026), https://doi.org/10.1016/j.xplc.2026.101714

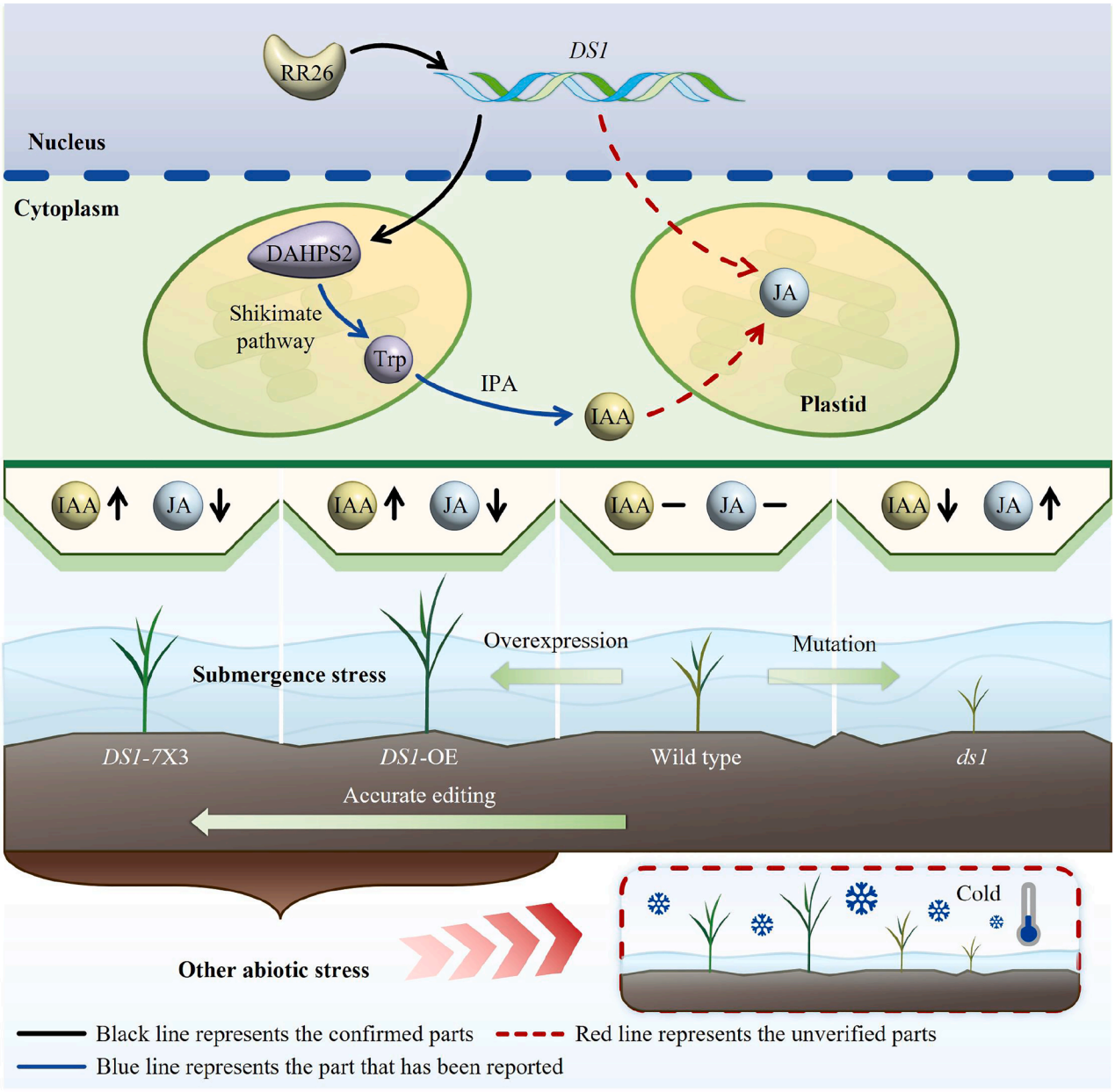

Figure 7. Proposed model of *DS1*-mediated hormonal homeostasis regulating submergence tolerance.

DS1, positively regulated by the type-B CK response regulator RR26, encodes DAHPS2, the first enzyme of the shikimate pathway, which supplies Trp for Trp-dependent IAA biosynthesis. In *ds1* mutants, reduced IAA levels and excessive JA accumulation inhibit postgermination growth and lead to pleiotropic developmental defects. In WT plants, *DS1* maintains IAA–JA balance, supporting normal growth but conferring limited submergence tolerance. In *DS1*-overexpressing (*DS1*-OE) and precisely edited (*DS1*-7X3) plants, elevated IAA levels and suppressed JA accumulation promote robust postgermination growth and significantly improve submergence tolerance. Black lines represent experimentally validated pathways, blue lines indicate previously reported pathways, and red lines represent putative or unverified regulatory relationships.

SUB1A, suppresses growth under submergence by coordinately reducing IAA levels and elevating JA accumulation (Xu et al., 2006; Khalil et al., 2024). In contrast, the escape strategy actively suppresses JA activity to promote coleoptile elongation, as demonstrated by the glucosyltransferase OsUGT75A, which reduces JA and ABA levels to facilitate rapid coleoptile growth (He et al., 2023). Our findings position DS1 upstream of these regulatory layers, functioning at the metabolic level to sustain IAA production while simultaneously limiting JA accumulation, thereby creating a permissive hormonal environment for rapid postgermination growth.

Moreover, we identified the type-B CK response regulator RR26 as a transcriptional activator of *DS1* (Figures 5A–5F), linking CK signaling with the shikimate pathway and IAA–JA homeostasis. CK accumulation is known to inhibit auxin signaling and root development (Li et al., 2024), suggesting that CK may also influence coleoptile elongation through interactions with IAA,

Please cite this article in press as: Chen et al., Prime editing of an RR26-responsive *cis*-element enhances *DAHPS2* expression and submergence tolerance in rice through the shikimate pathway, Plant Communications (2026), https://doi.org/10.1016/j.xplc.2026.101714

similar to the antagonistic relationship between IAA and JA. Given that the shikimate pathway also supplies precursors for SA biosynthesis, DS1 may further influence SA homeostasis. Together with previously characterized regulators such as *SUB1A*, which integrates ethylene, GA, brassinosteroid, JA, and auxin responses during the quiescence strategy, and *OsUGT75A*, which modulates JA and ABA during escape growth, *DS1* emerges as a pivotal hub mediating crosstalk among multiple phytohormonal pathways, including IAA, JA, CK, and potentially SA. These regulatory nodes collectively function as molecular bridges that fine-tune hormonal interactions and coordinate postgermination growth in rice. The precise mechanisms underlying this multi-hormonal integration remain to be elucidated. Notably, the key germination-related hormones GA and ABA do not appear to be directly influenced by DS1, which likely explains why *DS1* mutations did not significantly affect seed germination rates (Supplemental Figures 1A–1C).

DS1 overexpression enhances postgermination growth to counteract multiple stresses

In modern rice production systems, there is a growing shift from traditional seedling raising and transplanting toward simplified, labor-saving cultivation methods. Among these, dry and wet direct seeding have been increasingly adopted due to their reduced labor requirements and improved operational efficiency. However, most elite rice cultivars were bred for conventional transplanting systems and consequently exhibit poor submergence tolerance and slow early seedling growth under direct-seeding conditions. These limitations often result in uneven emergence, patchy seedling establishment, and asynchronous crop development under large-scale mechanized sowing, ultimately reducing production efficiency and constraining the broader application of direct-seeding technologies. Therefore, the development of submergence-tolerant rice germplasm specifically optimized for direct seeding is essential for integrating genetic improvement with modern agronomic practices, reducing production costs, and enhancing overall yield potential.

During the postgermination stage, overexpression of *DS1* in the HZ background (*DS1*-OE/HZ) caused elevated IAA levels and substantially reduced JA accumulation in the coleoptile and first incomplete leaf compared with the WT/HZ (Figures 4B and 4C). These hormonal alterations promoted vigorous postgermination growth and conferred enhanced submergence tolerance under both laboratory and field conditions (Figures 4D–4J). Similarly, *DS1* overexpression in the *japonica* cultivar ZJ3 also enhanced submergence tolerance (Supplemental Figures 9A–9C), indicating that the positive effect of *DS1* overexpression is conserved across different genetic backgrounds. Notably, under combined cold and submergence stress, *DS1*-OE/HZ lines maintained a pronounced growth advantage under both laboratory and field conditions (Supplemental Figures 10A–10D and 11A–11J). These results indicate that *DS1* overexpression enhances postgermination growth vigor, enabling direct-seeded rice to overcome multiple establishment constraints imposed by heterogeneous field conditions—including waterlogging, seed desiccation, and low-temperature stress—and thereby markedly improving seedling emergence rates.

Furthermore, IAA and JA contents in flag leaves at the heading stage were comparable between *DS1*-OE/HZ and WT/HZ plants (Supplemental Figures 18A and 18B), suggesting that *DS1 overexpression does not* disrupt hormone homeostasis at later developmental stages. Consistently, *DS1-OE/HZ plants* showed no obvious phenotypic differences from WT/HZ at the heading stage (Supplemental Figure 19A). Compared with WT/HZ, *DS1*-OE/HZ lines exhibited slight decreases in plant height, number of secondary branches, seed-setting rate, and thousand-grain weight, accompanied by modest increases in tiller number, panicle length, and number of primary branches (Supplemental Figure 19B). No significant differences were observed in grain number per panicle, grain length, or grain width (Supplemental Figure 19B). Overall, yield per plant was not significantly affected (Supplemental Figure 19C). Similarly, no adverse effects on agronomic traits were observed in *DS1*-OE/ZJ3 lines (Supplemental Figures 20A–20I). These results indicate that *DS1* overexpression promotes postgermination growth rate in rice without compromising subsequent plant growth, development, or yield potential.

DS1 regulatory elements represent a potential strategy for improving submergence tolerance in direct-seeded rice

Given that elevated *DS1* expression enhances submergence tolerance, we next sought to identify upstream transcriptional regulators controlling *DS1* expression during the postgermination stage. We identified RR26, a type-B CK response regulator, as a positive regulator of *DS1*. Increasing the copy number of the RR26-binding motif *DS1-7* in promoter–reporter assays resulted in a dose-dependent increase in LUC/REN ratios (Figure 6B). The *rr26* mutant exhibited postgermination growth defects similar to those observed in *ds1* (Supplemental Figures 14A–14D), and these defects were partially alleviated by exogenous application of NAA or the JA biosynthesis inhibitor DIECA (Figures 5J–5O). Moreover, DS1 transcript levels were significantly upregulated in *RR26*-OE/NIP lines, which exhibited markedly improved submergence tolerance compared with WT/NIP plants (Figures 5G–5I).

Analysis of natural variation in the *DS1* promoter identified four haplotypes that showed clear divergence between *indica* and *japonica* cultivars (Supplemental Figure 15A). However, neither DS1 transcript abundance nor promoter activity differed significantly among these haplotypes (Supplemental Figures 15B and 15C), indicating that natural polymorphisms within this region have limited impact on *DS1* expression. We therefore selected the *DS1-7* element as the optimal target for precise editing using the ePE2 prime editing system (Li et al., 2023b; Zou et al., 2025). Targeted modification of the *DS1* promoter generated transgene-free rice lines with enhanced *DS1* expression and improved submergence tolerance (Figures 6C–6F), without detectable developmental abnormalities at later growth stages (Supplemental Figures 16A–16G). These edited germplasm lines have substantial breeding potential. The *indica* rice cultivar HZ, an elite restorer line widely used in hybrid rice production in China, was selected as the editing background due to its agronomic importance. To date, HZ has contributed to the development of more than 300 hybrid rice cultivars, cumulatively cultivated over 300 million mu (~20 million hectares), making it an ideal candidate for improving stress resilience via precise genetic modification.

Please cite this article in press as: Chen et al., Prime editing of an RR26-responsive *cis*-element enhances *DAHPS2* expression and submergence tolerance in rice through the shikimate pathway, Plant Communications (2026), https://doi.org/10.1016/j.xplc.2026.101714

In summary, *DS1* overexpression significantly enhances postgermination growth and represents a promising molecular target for improving seedling establishment under submergence in direct-seeded rice systems. Targeted editing of the *DS1-7 regulatory element provides a precise, transgene-free strategy for enhancing submergence tolerance.* Future studies should focus on elucidating how *DS1* expression is adaptively regulated across diverse ecological environments and on dissecting its crosstalk with other hormone signaling pathways. These efforts will further advance molecular breeding strategies for developing high-yielding, submergence-tolerant rice cultivars tailored to direct-seeded agricultural systems.

METHODS

Plant materials and growth assays

The *ds1* mutants were generated by ethyl methane sulfonate mutagenesis of the *indica* rice (*Oryza sativa* L.) cultivar HZ. An F_2 segregating population, obtained by crossing heterozygous *ds1* plants with the *japonica* cultivar WYG7, was used to fine map the *DS1* gene. Unless otherwise indicated, all plants were grown in paddy fields under natural conditions at the China National Rice Research Institute in Fuyang, Zhejiang Province, China (119° 6′ E, 30° 0′ N).

For GUS staining in *ds1* plants containing *DR5:GUS* (Ulmasov et al., 1997), heterozygous *ds1* plants were crossed with the *japonica* cultivar 'Dongjing' carrying *DR5:GUS* (Yu et al., 2015), generating *ds1* mutants harboring *DR5:GUS*.

For laboratory submergence assays, mature seeds of WT/HZ and *DS1*-OE/HZ, WT/ZJ3 and *DS1*-OE/ZJ3, WT/NIP and *RR26*-OE/NIP, as well as WT/HZ and *DS1-7*X3/HZ were sown in transparent glass culture flasks containing 5 cm of water and incubated at 26°C under a 14-h light/10-h dark photoperiod for 7–10 days.

For field submergence assays, WT/HZ and *DS1*-OE/HZ seeds were directly sown in paddy fields in Fuyang, Zhejiang Province, and in Lingshui, Hainan Province, China (109° 55′ E, 18° 47′ N), where they were submerged to a depth of 5 cm for 23–25 days.

Seed germination assays

To overcome the sterility of homozygous *ds1* mutants, a half-seed strategy was employed. Mature seeds harvested from heterozygous *ds1* plants were bisected, with the endosperm-containing half used for genomic DNA extraction and the corresponding embryo-containing half reserved for subsequent phenotypic and molecular analyses. Homozygous *ds1* mutants were identified by amplifying the target region with primers DS1Msite-F (5′-CTCGATGGAGCTCATGTTGA-3′) and DS1Msite-R (5′-CCCAGTTTCT TTTCCCTTCC-3′), followed by high-throughput sequencing using the high-throughput tracking of mutations (Hi-TOM) platform. Only seeds confirmed as homozygous *ds1* mutants were used in subsequent experiments. For quantitative germination assays, 50 seeds each of WT and homozygous *ds1* mutants were evaluated per replicate. Seed coats were removed and seeds were cut into halves prior to the assay. Germination was defined as the emergence of the coleoptile to a length equivalent to that of the halved seed. Germination status was recorded at 12-h intervals.

Map-based cloning

Over 2100 mutant individuals were selected from a population of 16 300 F_2 plants derived from the cross between heterozygous *ds1* plants and WYG7. Genomic DNA was extracted using the cetyl trimethylammonium bromide method (Stewart and Via, 1993). Simple sequence repeat and sequence-tagged site markers showing polymorphisms between HZ and WYG7 were used for *DS1* mapping. PCR products were separated on 4%–5% agarose gels. Candidate genes within the target interval were amplified and sequenced by Hangzhou Tsingke Biological Engineering Technology and Service. Primers used for fine mapping and sequencing are listed in Supplemental Table 1, and predicted genes within the mapped region are listed in Supplemental Table 2.

Vector construction and genetic transformation

For mutant complementation, a 6988-bp genomic DNA fragment containing 2749-bp upstream of the start codon, the 3239 bp *DS1* coding sequence, and 1000 bp downstream was amplified using primers DS1COMF/R and cloned into pCAMBIA1300, generating pCAMBIA1300-DS1COM (DS1COM). The control vector and DS1COM construct were introduced into HZ and heterozygous *ds1* plants via *Agrobacterium*-mediated transformation.

For gene knockout, two target sequences in *DS1,* 5'-TTCATGGATC ACAGCGAACA-3' (cas1) and 5'-TACAGGGGAGACAACATCAA-3' (cas2), and one target sequence in *RR26,* TCGAGGATCTTGAGCCAGGT, were designed. Deletion vectors were constructed using the CRISPR–Cas9 system (Wang et al., 2017) and introduced into NIP via *Agrobacterium*-mediated transformation.

For *DS1* overexpression, the full-length *DS1* coding sequence (excluding the termination codon) was amplified using primers DS1-GFPF/R, inserted into the pCAMBIA1300-GFP-FLAG vector, and transformed into HZ and ZJ3 via *Agrobacterium*-mediated transformation.

For prime editing, the ePE2 (pHUC411-cMYL-PEmaxNC) system was used to increase the copy number of the *DS1-7* promoter element in HZ, as described by Zou et al. (2025) and Li et al. (2023b). The resulting constructs were transformed into HZ or NIP via *Agrobacterium*-mediated transformation. Primers used for vector construction are listed in Supplemental Table 3.

Histological analysis

For paraffin sectioning, fresh leaves from three-leaf-stage seedlings, flag leaves, leaf cushions, and spikelets at the heading stage were collected and fixed in 50% Formalin-Acetic Acid-Alcohol solution (5% glacial acetic acid, 5% formaldehyde, and 70% ethanol). Samples were dehydrated through a graded ethanol series and embedded in paraffin. Sections of 5 μm thickness were prepared using a microtome (Leica), stained with toluidine blue, and observed under a microscope (Nikon 90i).

To analyze the expression pattern of *DS1*, a 2749-bp promoter fragment was amplified from HZ genomic DNA and cloned upstream of the GUS reporter gene in the pCAMBIA1305 binary vector. The resulting plasmid was introduced into HZ to generate transgenic plants. For GUS staining, 8-cm root tips from three-leaf stage *DS1*-GUS T_1 transgenic plants, HZ, and *ds1* mutants containing *DR5:GUS* were infiltrated with GUS staining solution and incubated at 37°C overnight. Samples were then dehydrated through a graded ethanol series and embedded in ethanol. Primers used for GUS vector construction are listed in Supplemental Table 3.

RNA extraction and RT-qPCR

Total RNA was extracted from various tissues using an AxyPrep Total RNA Miniprep Kit (Axygen). First-strand cDNA was synthesized using RevertAce quantitative PCR RT Master Mix (Toyobo) following the manufacturer's instructions. RT-qPCR was performed on a CFX96 Touch Real-Time PCR Detection System (Bio-Rad) using 2× SsoFast EvaGreen SuperMix. *OsUBQ5* and *OsActin* were used as internal reference genes. Data are presented as mean ± SD from three biological replicates, and statistical significance was evaluated using Student's *t*-test. Primers used for RT-qPCR are listed in Supplemental Table 4.

Endogenous hormone content and DS1 enzyme activity measurement

Coleoptiles and first incomplete leaves (approximately 0.1 g fresh weight) from WT, *ds1*, and *DS1*-OE lines at the postgermination stage, as well as

Please cite this article in press as: Chen et al., Prime editing of an RR26-responsive *cis*-element enhances *DAHPS2* expression and submergence tolerance in rice through the shikimate pathway, Plant Communications (2026), https://doi.org/10.1016/j.xplc.2026.101714

flag leaves from WT and *DS1*-OE lines at the heading stage, were collected and ground in liquid nitrogen. IAA and JA contents were determined by high performance liquid chromatography (Waters Xevo-TQD) as described by Pan et al. (2010).

For DS1 enzyme activity assays, plasmids expressing different *DS1* variants were introduced into *Escherichia coli* strain BL21 (DE3). Cultures grown at 37°C were induced with 0.2 mM isopropyl-β-D-thiogalactopyranoside at 18°C for 16 h. Bacterial cells were harvested, sonicated in 1× PBS (pH 7.4) and centrifuged at 12 000 rpm for 10 min. The supernatant was used to measure DAHPS enzyme activity using an ELISA kit (MM-62834O2, Jiangsu Meimian Industrial). Each sample was analyzed with four biological replicates.

Subcellular localization

Full-length cDNAs of *DS1* and *RR26* were amplified and fused into the pCAMBIA1300-GFP-FLAG vector under the control of the Ubi promoter. Rice protoplasts were isolated and transformed as described previously (Qiu et al., 2016), then incubated at 28°C for 14–16 h. GFP fluorescence was detected using a confocal laser scanning microscope (Carl Zeiss LSM 980).

Phylogenetic analysis

Protein sequences used for phylogenetic analysis were identified by BLASTP searches using DS1 and RR26 as queries. Full-length amino acid sequences were aligned using DNAMAN software. Phylogenetic trees were constructed using the neighbor-joining method in MEGA (v7), with bootstrap analysis based on 1000 replicates.

Hormone response assays

Dehulled seeds containing embryos were surface-sterilized by immersion in 70% (v/v) ethanol for 1 min, rinsed twice, incubated in 10% NaClO for 30 min, and thoroughly washed with sterile water. Sterilized seeds were sown on half-strength Murashige and Skoog (1/2 MS) medium supplemented with 5 nM NAA (a synthetic auxin analog), 5 nM NPA (an auxin efflux inhibitor), 5 μM JA, or 5 μM DIECA (a JA biosynthesis inhibitors), or no chemical treatment as a control. Coleoptile and radicle lengths were measured on day 5 and the plants were photographed.

For hydroponic hormone treatments, WT and *ds1* seedlings were grown to the three-leaf stage and treated with either 20 μM IAA or 50 μM yucasin, a specific inhibitor of YUCCA-dependent auxin biosynthesis (5-(4-chlorophenyl)-4H-1,2,4-triazole-3-thiol), or double-distilled water as a control for 7 days. Root lengths were then measured and documented.

LUC assays

For LUC activity assays in rice protoplasts, different lengths of the *DS1* promoter were cloned into the pGreen0800-LUC reporter vector, and the full-length *RR26* cDNA was cloned into pCAMBIA1300-GFP-FLAG as an effector. These plasmids were co-transformed into rice protoplasts and incubated at 28°C for 16–18 h. LUC and REN activities were measured using the Dual-Luciferase Reporter Assay System (Promega) following the manufacturer's protocol.

For LUC activity assays in tobacco, plasmids were infiltrated into *Nicotiana benthamiana* leaves via *Agrobacterium tumefaciens*. After 48–72 h, luminescence signals were detected using a low-light cooled imaging apparatus (Tanon 5200). Primers used for these assays are listed in Supplemental Table 3.

Y1H assay

For Y1H analysis, the full-length cDNA of *RR26* was cloned into the pB42AD vector, and different fragments of the *DS1* promoter were inserted into pLacZi2u carrying the LacZ reporter gene. The resulting constructs were co-transformed into the yeast strain EGY48. Y1H assays were performed using the Clontech Y1H system (Takara, Beijing, China) following the manufacturer's instructions. Primers used for construct generation are listed in Supplemental Table 3.

EMSA

For EMSA, a 1299 bp C-terminal fragment of *RR26* was cloned into a maltose-binding protein (MBP) fusion vector. The recombinant *RR26*-MBP plasmid and an empty MBP vector as a control were transformed into *Escherichia coli* strain BL21 (DE3). Cultures were grown at 37°C and induced with 0.2 mM isopropyl-β-D-thiogalactopyranoside at 18°C for 16 h. Fusion proteins were purified using MBP agarose according to the manufacturer's protocol. Biotin-labeled and unlabeled DNA probes were synthesized by Sunya Biological Technology. DNA-binding reactions were performed in EMSA/gel-shift binding buffer (Beyotime, GS005) at room temperature for 20 min. Reaction mixtures were separated on a 4% native polyacrylamide gel and transferred to a nylon membrane. Fluorescence signals were detected using a chemiluminescent EMSA kit (Beyotime, GS009) according to the manufacturer's protocol. Competitive binding assays with increasing amounts of unlabeled probes were conducted to determine protein–DNA interaction specificity. Purified MBP protein was used as a negative control.

Statistical analysis

Statistical significance was evaluated using Student's *t*-test for comparisons between two groups. Significance thresholds were set at $P < 0.05$ and $P < 0.01$. Quantitative data are presented as means ± SD from at least three independent biological replicates. Statistical analyses were performed using GraphPad Prism (v8.4.2).

DATA AND CODE AVAILABILITY

All materials generated in this study are available from the corresponding author upon reasonable request.

FUNDING

This work was supported by the National Key Research and Development Program of China (2023YFF1001200); the National Natural Science Foundation of China (32188102, 32201784, and 32072048); the Biological Breeding–National Science and Technology Major Project (2024ZD04077); the Hainan Province Key Research and Development Program (ZDYF2024HXGG005); the Innovation Platform for Academicians of Hainan Province (YSPTZX2502); the Agricultural Science and Technology Innovation Program (ASTIP) and CAAS-ZDRW202401; and the Agricultural Science and Technology Major Project and Academician Workstation of the National Nanfan Research Institute (Sanya), CAAS (YBXM2526 and YBXM2527).

ACKNOWLEDGMENTS

We thank Kejian Wang and Chun Wang for providing the ePE2 system, and Qing Liu for access to the Hi-TOM sequencing platform. We express our gratitude to colleagues and collaborators for their contributions of materials and technical assistance, including Yuexing Wang, Huimei Wang, Lin Wang, Qunen Liu, Jian Zhang, and Jinpeng Zou (China National Rice Research Institute); Yanhua Qi (Inner Mongolia University); Zhigang Zhao (Nanjing Agricultural University); Chengbin Xiang (University of Science and Technology of China); and Zhixuan Sun (The Village School Houston). We also thank the Public Laboratory of China National Rice Research Institute for technical support with paraffin sectioning and endogenous hormone measurements. The authors declare no conflicts of interest.

AUTHOR CONTRIBUTIONS

L.Z. and Q.Q. conceived and designed the experiments. D.C., L.H., Z.Q., Q.W., M.L., Z.H., and P.D. performed the experiments and conducted bioinformatic analyses. Q.X., G.Z., J.H., Z.G., G.D., D.R., L.S., Y.R., Q.L., Y.Z., Q.Z., L.G., and L.S. analyzed the data. D.C., L.H., and Z.Q. wrote the manuscript. L.Z., L.S., and Q.Q. revised the manuscript.

DECLARATION OF GENERATIVE AI AND AI-ASSISTED TECHNOLOGIES IN THE WRITING PROCESS

During manuscript preparation, the authors used ChatGPT-5 and DeepSeek to improve language clarity and readability. All content was subsequently reviewed and edited by the authors, who take full responsibility for the final manuscript.

SUPPLEMENTAL INFORMATION

Supplemental information is available at *Plant Communications Online*.

Received: November 18, 2025
Revised: January 5, 2026
Accepted: January 8, 2026

REFERENCES

Bailey-Serres, J., Lee, S.C., and Brinton, E. (2012). Waterproofing crops: effective flooding survival strategies. Plant Physiol. **160**:1698–1709. https://doi.org/10.1104/pp.112.208173.

Casanova-Sáez, R., Mateo-Bonmatí, E., and Ljung, K. (2021). Auxin metabolism in plants. Cold Spring Harbor Perspect. Biol. **13**:a039867. https://doi.org/10.1101/cshperspect.a039867.

Chen, J., Zhu, M., Liu, R., Zhang, M., Lv, Y., Liu, Y., Xiao, X., Yuan, J., and Cai, H. (2020). BIOMASS YIELD 1 regulates sorghum biomass and grain yield via the shikimate pathway. J. Exp. Bot. **71**:5506–5520. https://doi.org/10.1093/jxb/eraa275.

Chen, Q., Sun, J., Zhai, Q., Zhou, W., Qi, L., Xu, L., Wang, B., Chen, R., Jiang, H., Qi, J., et al. (2011). The basic helix-loop-helix transcription factor MYC2 directly represses *PLETHORA* expression during jasmonate-mediated modulation of the root stem cell niche in *Arabidopsis*. Plant Cell **23**:3335–3352. https://doi.org/10.1105/tpc.111.089870.

Dathe, W., Rönsch, H., Preiss, A., Schade, W., Sembdner, G., and Schreiber, K. (1981). Endogenous plant hormones of the broad bean, *Vicia faba* L. (-)-Jasmonic acid, a plant growth inhibitor in pericarp. Planta **153**:530–535. https://doi.org/10.1007/BF00385537.

Entus, R., Poling, M., and Herrmann, K.M. (2002). Redox regulation of Arabidopsis 3-deoxy-d-*arabino*-heptulosonate 7-phosphate synthase. Plant Physiol. **129**:1866–1871. https://doi.org/10.1104/pp.002626.

Farmer, E.E., Caldelari, D., Pearce, G., Walker-Simmons, M.K., and Ryan, C.A. (1994). Diethyldithiocarbamic acid inhibits the octadecanoid signaling pathway for the wound induction of proteinase inhibitors in tomato leaves. Plant Physiol. **106**:337–342. https://doi.org/10.1104/pp.106.1.337.

Gosset, G., Bonner, C.A., and Jensen, R.A. (2001). Microbial origin of plant-type 2-keto-3-deoxy-D-*arabino*-heptulosonate 7-phosphate synthases, exemplified by the chorismate- and tryptophan-regulated enzyme from *Xanthomonas campestris*. J. Bacteriol. **183**:4061–4070. https://doi.org/10.1128/JB.183.13.4061-4070.2001.

Herrmann, K.M., and Weaver, L.M. (1999). The shikimate pathway. Annu. Rev. Plant Biol. **50**:473–503. https://doi.org/10.1146/annurev.arplant.50.1.473.

He, Y., Sun, S., Zhao, J., Huang, Z., Peng, L., Huang, C., Tang, Z., Huang, Q., and Wang, Z. (2023). UDP-glucosyltransferase OsUGT75A promotes submergence tolerance during rice seed germination. Nat. Commun. **14**:2296. https://doi.org/10.1038/s41467-023-38085-5.

Hsu, S.K., and Tung, C.W. (2015). Genetic mapping of anaerobic germination-associated QTLs controlling coleoptile elongation in rice. Rice **8**:38. https://doi.org/10.1186/s12284-015-0072-3.

Huang, C., He, Y., Li, W., Liu, L., Wu, Z., Zhong, Y., Wang, C., Peng, L., Sun, S., Huang, Z., et al. (2025). Feedback transcription regulation between OsNAC3 and OsDREB1A promotes postgermination growth in rice. Sci. Adv. **11**:eadw0421. https://doi.org/10.1126/sciadv.adw0421.

Huang, C.F., Yu, C.P., Wu, Y.H., Lu, M.Y.J., Tu, S.L., Wu, S.H., Shiu, S.H., Ku, M.S.B., and Li, W.H. (2017). Elevated auxin biosynthesis and transport underlie high vein density in C_4 leaves. Proc. Natl. Acad. Sci. USA **114**:E6884–E6891. https://doi.org/10.1073/pnas.1709171114.

Inada, N., Sakai, A., Kuroiwa, H., and Kuroiwa, T. (2002). Three-dimensional progression of programmed death in the rice coleoptile. Int. Rev. Cytol. **218**:221–258. https://doi.org/10.1016/s0074-7696(02)18014-4.

Kanna, S., Mase, K., Nakano, Y., Nishikubo, N., Sugita, R., Tsuboi, Y., Kajita, S., Zhou, J., Kitano, H., and Katayama, Y. (2006). 3-Deoxy-D-*arabino*-heptulosonate 7-phosphate synthase is regulated for the accumulation of polysaccharide-linked hydroxycinnamoyl esters in rice (*Oryza sativa* L.) internode cell walls. Plant Cell Rep. **25**:676–688. https://doi.org/10.1007/s00299-006-0124-7.

Khalil, M.I., Hassan, M.M., Samanta, S.C., Chowdhury, A.K., Hassan, M.Z., Ahmed, N.U., Somaddar, U., Ghosal, S., Robin, A.H.K., Nath, U.K., et al. (2024). Unraveling the genetic enigma of rice submergence tolerance: Shedding light on the role of ethylene response factor-encoding gene *SUB1A-1*. Plant Physiol. Biochem. **206**:108224. https://doi.org/10.1016/j.plaphy.2023.108224.

Li, X., Dong, J., Zhu, W., Zhao, J., and Zhou, L. (2023a). Progress in the study of functional genes related to direct seeding of rice. Mol. Breed. **43**:46. https://doi.org/10.1007/s11032-023-01388-y.

Li, J., Ding, J., Zhu, J., Xu, R., Gu, D., Liu, X., Liang, J., Qiu, C., Wang, H., Li, M., et al. (2023b). Prime editing-mediated precise knockin of protein tag sequences in the rice genome. Plant Commun. **4**:100572. https://doi.org/10.1016/j.xplc.2023.100572.

Li, L., Jia, L., Duan, X., Lv, Y., Ye, C., Ding, C., Zhang, Y., Qi, W., Motte, H., Beeckman, T., et al. (2024). A nitrogen-responsive cytokinin oxidase/dehydrogenase regulates root response to high ammonium in rice. New Phytol. **244**:1391–1407. https://doi.org/10.1111/nph.20128.

Maeda, H., and Dudareva, N. (2012). The shikimate pathway and aromatic amino acid biosynthesis in plants. Annu. Rev. Plant Biol. **63**:73–105. https://doi.org/10.1146/annurev-arplant-042811-105439.

Narsai, R., Edwards, J.M., Roberts, T.H., Whelan, J., Joss, G.H., and Atwell, B.J. (2015). Mechanisms of growth and patterns of gene expression in oxygen-deprived rice coleoptiles. Plant J. **82**:25–40. https://doi.org/10.1111/tpj.12786.

Nishimura, T., Hayashi, K.I., Suzuki, H., Gyohda, A., Takaoka, C., Sakaguchi, Y., Matsumoto, S., Kasahara, H., Sakai, T., Kato, J.I., et al. (2014). Yucasin is a potent inhibitor of YUCCA, a key enzyme in auxin biosynthesis. Plant J. **77**:352–366. https://doi.org/10.1111/tpj.12399.

Pan, X., Welti, R., and Wang, X. (2010). Quantitative analysis of major plant hormones in crude plant extracts by high-performance liquid chromatography-mass spectrometry. Nat. Protoc. **5**:986–992. https://doi.org/10.1038/nprot.2010.37.

Pucciariello, C. (2020). Molecular mechanisms supporting rice germination and coleoptile elongation under low oxygen. Plants **9**:1037. https://doi.org/10.3390/plants9081037.

Qiao, J., Quan, R., Wang, J., Li, Y., Xiao, D., Zhao, Z., Huang, R., and Qin, H. (2024). OsEIL1 and OsEIL2, two master regulators of rice ethylene signaling, promote the expression of ROS scavenging genes to facilitate coleoptile elongation and seedling emergence from soil. Plant Commun. **5**:100771. https://doi.org/10.1016/j.xplc.2023.100771.

Qiu, J., Hou, Y., Tong, X., Wang, Y., Lin, H., Liu, Q., Zhang, W., Li, Z., Nallamilli, B.R., and Zhang, J. (2016). Quantitative phosphoproteomic analysis of early seed development in rice (*Oryza sativa* L.). Plant Mol. Biol. **90**:249–265. https://doi.org/10.1007/s11103-015-0410-2.

Richards, T.A., Dacks, J.B., Campbell, S.A., Blanchard, J.L., Foster, P.G., McLeod, R., and Roberts, C.W. (2006). Evolutionary origins of the eukaryotic shikimate pathway: gene fusions, horizontal gene transfer, and endosymbiotic replacements. Eukaryot. Cell **5**:1517–1531. https://doi.org/10.1128/EC.00106-06.

Shang, L., Li, X., He, H., Yuan, Q., Song, Y., Wei, Z., Lin, H., Hu, M., Zhao, F., Zhang, C., et al. (2022). A super pan-genomic landscape of rice. Cell Res. **32**:878–896. https://doi.org/10.1038/s41422-022-00685-z.

Stewart, C.N., Jr., and Via, L.E. (1993). A rapid CTAB DNA isolation technique useful for RAPD fingerprinting and other PCR applications. Biotechniques **14**:748–750. https://www.ncbi.nlm.nih.gov/pubmed/8512694.

Sun, S., Wang, T., Wang, L., Li, X., Jia, Y., Liu, C., Huang, X., Xie, W., and Wang, X. (2018). Natural selection of a *GSK3* determines rice mesocotyl domestication by coordinating strigolactone and brassinosteroid signaling. Nat. Commun. **9**:2523. https://doi.org/10.1038/s41467-018-04784-7.

Tan, X., Calderon-Villalobos, L.I.A., Sharon, M., Zheng, C., Robinson, C.V., Estelle, M., and Zheng, N. (2007). Mechanism of auxin perception by the TIR1 ubiquitin ligase. Nature **446**:640–645. https://doi.org/10.1038/nature05731.

Tohge, T., Watanabe, M., Hoefgen, R., and Fernie, A.R. (2013). Shikimate and phenylalanine biosynthesis in the green lineage. Front. Plant Sci. **4**:62. https://doi.org/10.3389/fpls.2013.00062.

Tzin, V., and Galili, G. (2010). The biosynthetic pathways for shikimate and aromatic amino acids in *Arabidopsis thaliana*. Arabidopsis Book **8**:e0132–e1298. https://doi.org/10.1199/tab.0132.

Ulmasov, T., Hagen, G., and Guilfoyle, T.J. (1997). ARF1, a transcription factor that binds auxin response elements. Science **276**:1865–1868. https://doi.org/10.1126/science.276.5320.1865.

Wang, H., Shi, Y., Zhang, X., Xu, X., and Wu, J.L. (2020). Characterization of a novel rice dynamic narrow-rolled leaf mutant with deficiencies in aromatic amino acids. Int. J. Mol. Sci. **21**:1521. https://doi.org/10.3390/ijms21041521.

Wang, Y., Jin, G., Song, S., Jin, Y., Wang, X., Yang, S., Shen, X., Gan, Y., Wang, Y., Li, R., et al. (2024). A peroxisomal cinnamate:CoA ligase-dependent phytohormone metabolic cascade in submerged rice germination. Dev. Cell **59**:1363–1378.e4. https://doi.org/10.1016/j.devcel.2024.03.023.

Wang, Z.w., Lv, J., Xie, S.z., Zhang, Y., Qiu, Z.n., Chen, P., Cui, Y.t., Niu, Y.f., Hu, S.k., Jiang, H.z., et al. (2017). *OsSLA4* encodes a pentatricopeptide repeat protein essential for early chloroplast development and seedling growth in rice. Plant Growth Regul. **84**:249–260. https://doi.org/10.1007/s10725-017-0336-6.

Webby, C.J., Baker, H.M., Lott, J.S., Baker, E.N., and Parker, E.J. (2005). The structure of 3-deoxy-D-*arabino*-heptulosonate 7-phosphate synthase from *Mycobacterium tuberculosis* reveals a common catalytic scaffold and ancestry for type I and type II enzymes. J. Mol. Biol. **354**:927–939. https://doi.org/10.1016/j.jmb.2005.09.093.

Xu, K., Xu, X., Fukao, T., Canlas, P., Maghirang-Rodriguez, R., Heuer, S., Ismail, A.M., Bailey-Serres, J., Ronald, P.C., and Mackill, D.J. (2006). *Sub1A* is an ethylene-response-factor-like gene that confers submergence tolerance to rice. Nature **442**:705–708. https://doi.org/10.1038/nature04920.

Yamamoto, M., and Yamamoto, K.T. (1998). Differential effects of 1-naphthaleneacetic acid, indole-3-acetic acid and 2,4-dichlorophenoxyacetic acid on the gravitropic response of roots in an auxin-resistant mutant of Arabidopsis, *aux1*. Plant Cell Physiol. **39**:660–664. https://doi.org/10.1093/oxfordjournals.pcp.a029419.

Yokoyama, R., de Oliveira, M.V.V., Kleven, B., and Maeda, H.A. (2021). The entry reaction of the plant shikimate pathway is subjected to highly complex metabolite-mediated regulation. Plant Cell **33**:671–696. https://doi.org/10.1093/plcell/koaa042.

Yu, C., Sun, C., Shen, C., Wang, S., Liu, F., Liu, Y., Chen, Y., Li, C., Qian, Q., Aryal, B., et al. (2015). The auxin transporter, OsAUX1, is involved in primary root and root hair elongation and in Cd stress responses in rice (*Oryza sativa* L.). Plant J. **83**:818–830. https://doi.org/10.1111/tpj.12929.

Zhao, Y. (2010). Auxin biosynthesis and its role in plant development. Annu. Rev. Plant Biol. **61**:49–64. https://doi.org/10.1146/annurev-arplant-042809-112308.

Zhao, Y. (2012). Auxin biosynthesis: a simple two-step pathway converts tryptophan to indole-3-acetic acid in plants. Mol. Plant **5**:334–338. https://doi.org/10.1093/mp/ssr104.

Zou, J., Meng, X., Hong, Z., Rao, Y., Wang, K., Li, J., Yu, H., and Wang, C. (2025). Cas9-PE: a robust multiplex gene editing tool for simultaneous precise editing and site-specific random mutation in rice. Trends Biotechnol. **43**:433–446. https://doi.org/10.1016/j.tibtech.2024.10.012.